JOC The Journal of Organic Chemistry

Article

pubs.acs.org/joc

Synthesis of Ferrocene Oxazoline N,O ligands and Their Application in Asymmetric Ethyl- and Phenylzinc Additions to Aldehydes

Chris Nottingham, Robert Benson, Helge Müller-Bunz, and Patrick J. Guiry*

Centre for Synthesis and Chemical Biology, School of Chemistry and Chemical Biology, University College Dublin, Belfield, Dublin 4, Ireland

Supporting Information

ABSTRACT: The synthesis of a range of novel *gem*-disubstituted ferrocene–oxazoline ligands and their application in both the asymmetric ethyl- and phenylzinc additions to aldehydes is reported. These studies reveal that *gem*-disubstitution of *i*-Pr-containing ferrocene oxazoline ligands results in increased enantioselectivity compared to their unsubstituted counterparts. Utilizing zinc catalysis, these ligands provided a wide range of secondary alcohols in yields of up to 93% with ee's of up to >99%. An interesting crystal structure of a ferrocene oxide–lithium tetramer showing lithium–nitrogen coordination in the solid state is also presented.

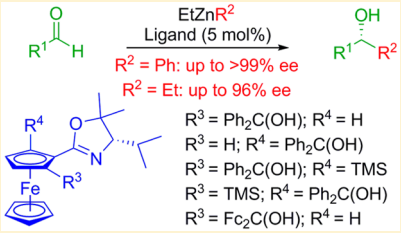

INTRODUCTION

Oxazoline ligands such as PHOX[1−3] represent a privileged ligand scaffold in transition-metal catalysis.[4−8] In most cases, *t*-Bu-PHOX ligands provide the highest ee's; however, the synthesis of these ligands involves starting from the expensive, non-natural amino acids (*S*)- and (*R*)-*tert*-leucine, which severely limits their application in asymmetric catalysis.[9] With this in mind, Paquin recently reported the synthesis and application of 5,5-(dimethyl)-*i*-Pr-PHOX as a cheaper, practical equivalent of the expensive *t*-Bu-PHOX.[10,11] This *gem*-disubstitution effect has recently been explored further by both our group[12,13] and the group of Stoltz[14] with excellent results in both cases. We sought to further investigate the general applicability of the *gem*-disubstitution effect with different oxazoline ligand architectures rather than the conventional PHOX type backbone. As an example, we have recently prepared series of a *gem*-disubstituted *i*-Pr HetPHOX ligands **1** and the *gem*-disubstituted FcPHOX ligand **2** and applied them in the asymmetric intermolecular Heck reaction, furnishing products in up to 98% yield with ee's of up to 97% (Figure 1).[12] In addition, we have prepared tridentate bis(oxazoline) ligands **3** and applied them in the zinc-catalyzed asymmetric Friedel–Crafts reaction, providing products with ee's of up to 95% (Figure 1).[13]

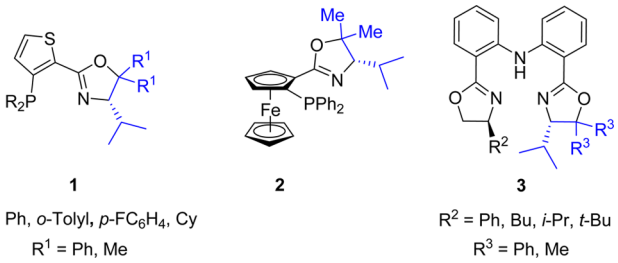

Figure 1. HetPHOX, FcPHOX and bis(oxazoline) ligands employing *gem*-disubstitution.

Continuing on from these studies, we wished to investigate the synthesis and application of a series of ferrocenyl hydroxyoxazoline ligands which are *gem*-dimethyl-substituted analogues of ligands previously developed by the groups of Bolm and Butenschön (Figure 2).[15,16]

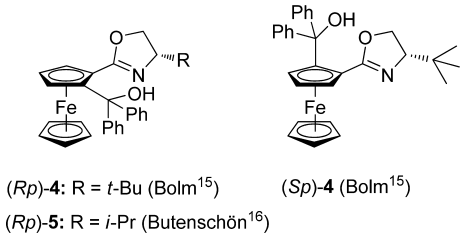

Figure 2. Bolm and Butenschön's ferrocenyl hydroxyoxazoline ligands.

With this in mind we designed disubstituted ferrocene ligands (R_p)-**6** and (S_p)-**6** (Figure 3). We planned to synthesize these N,O bidentate ligands from the cheap, natural amino acid (*S*)-valine. While both ligands contain the same central chirality, they differ in planar chirality. We also envisioned that the addition of a bulky TMS group *ortho* to the oxazoline ring could further influence the conformation of the oxazoline ring and may even direct the *i*-Pr group closer to the reaction center. This inspired the design of trisubstituted ligands (R_p)-7 and (S_p)-7, which would allow us to examine the conformational effects of an additional TMS group (Figure 3).

Furthermore, while many disubstituted ferrocene ligands have been applied in asymmetric catalysis, relatively few

Received: July 30, 2015
Published: September 1, 2015

DOI: 10.1021/acs.joc.5b01766
J. Org. Chem. 2015, 80, 10163−10176

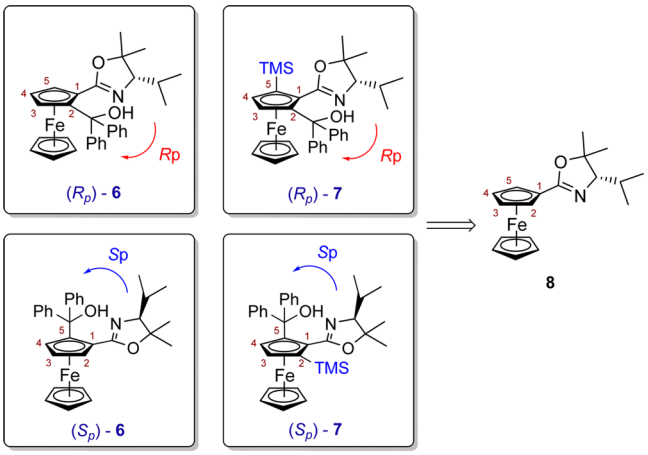

Figure 3. Ligand class **6** and **7** and key chiral precursor **8**.

trisubstituted ligands have been examined.[17,18] Previously, we have shown that trisubstituted ferrocenyl pyrrolidine ligands **9a–d** containing a TMS group perform differently than their disubstituted counterparts (Figure 4).[18]

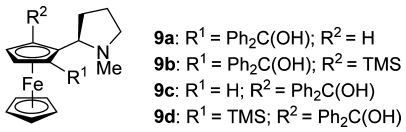

Figure 4. Ferrocenyl pyrrolidine ligands **9a–d**.

RESULTS AND DISCUSSION

Synthesis of Ligand Class 6 and 7. We have recently reported the high-yielding synthesis of key intermediate **8** starting from readily available (*S*)-valine methyl ester hydrochloride (Figure 3).[12] Based on this and previous work by Sammakia,[19] directed *ortho*-lithiation of **8** with *s*-BuLi and chelating agent tetramethylethylenediamine (TMEDA), followed by quenching with benzophenone, provided ligand (R_p)-**6** in 83% yield with a diastereomeric excess (de) of >99% (Scheme 1).

Scheme 1. Synthesis of Ligands (R_p)-6, (S_p)-6, and (S_p)-7[a]

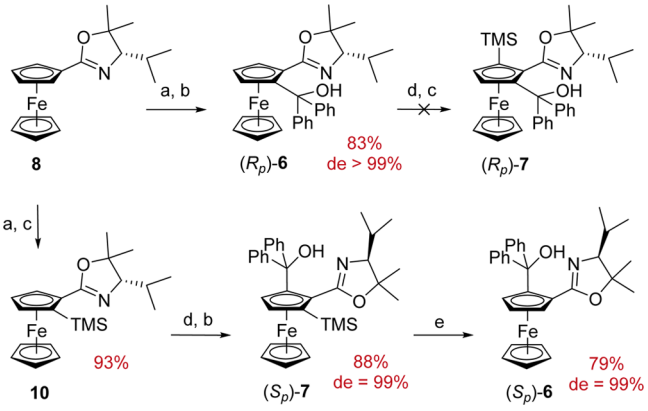

[a]Conditions: (a) *s*-BuLi, TMEDA, Et_2O, −78 °C, 10 min; (b) benzophenone, 0 °C to rt, 10 min; (c) TMSCl, 0 °C to rt, 10 min; (d) *n*-BuLi, Et_2O, −78 °C, 10 min; (e) TBAF, THF, reflux, 72 h.

Directed *ortho*-lithiation of **8** followed by quenching with TMSCl provided oxazoline **10** in 93% yield as a single diastereomer by ^{1}H NMR spectroscopy, which was then subjected to a second *ortho*-lithiation with *n*-BuLi and subsequent quench with benzophenone to provide the trisubstituted ferrocene oxazoline ligand (S_p)-**7** in 88% yield with 99% de. The TMS group was then removed from ligand (S_p)-**7** by exposure to tetrabutylammonium fluoride (TBAF) to provide disubstituted ferrocene oxazoline ligand (S_p)-**6** in 79% yield with 99% de (Scheme 1).

Originally, we thought that employing 2 equiv of a lithium base would allow successful deprotonation at the remaining *ortho*-position in ligand (R_p)-**6** to provide ligand (R_p)-**7** (Scheme 1). However, this was not successful and is likely due to the nitrogen of the oxazoline ring forming a seven-membered chelate ring with the lithium alkoxide formed upon alcohol deprotonation. This would lock the nitrogen in place and prevent directed *ortho*-metalation (DOM) by a second equivalent of base. The next logical step was to protect the alcohol group to determine if this allowed successful lithiation. However, the sterically hindered tertiary alcohol group proved unreactive using various protection protocols.[20] This was also the case with similar ligands (**9a–d**) where protection proved unsuccessful.[18] The choice of protecting group was also largely limited due to the fact that subsequent deprotection would have to take place without concomicant removal of the installed TMS group afterward. Due to these limitations, we decided to investigate an alternative route to ligand (R_p)-**7** that avoided protecting the hydroxy group (Scheme 2).

Scheme 2. Synthesis of Ligand (R_p)-7[a]

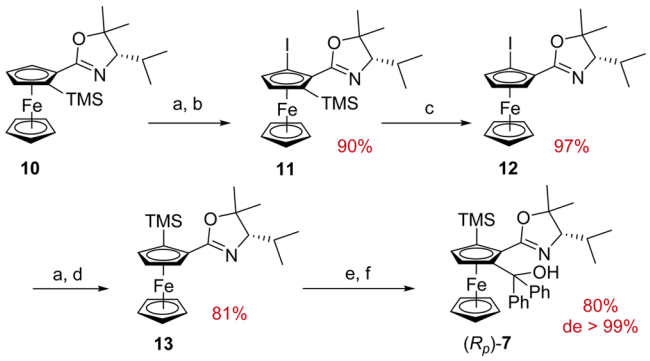

[a]Conditions: (a) *n*-BuLi, Et_2O, −78 °C, 10 min; (b) I_2, 0 °C to rt, 20 min; (c) TBAF, THF, reflux, 6 h; (d) TMSCl, 0 °C to rt, 10 min; (e) *s*-BuLi, TMEDA, Et_2O, −78 °C, 10 min; (f) benzophenone, 0 °C to rt, 10 min.

Ortho-lithiation of disubstituted ferrocene oxazoline **10** with *n*-BuLi and subsequent quenching with freshly sublimed iodine provided trisubstituted ferrocene **11** in 90% yield before subsequent deprotection utilizing TBAF to provide iodoferrocene **12** in 97% yield. Iodoferrocene **12** was then subjected to lithium–halogen exchange with *n*-BuLi and subsequently quenched with TMSCl to provide disubstituted ferrocene oxazoline **13** in 81% yield. A final directed *ortho*-lithiation with *s*-BuLi and TMEDA followed by quenching with benzophenone provided ligand (R_p)-**7** in 80% yield and >99% de (Scheme 2).

Revised Synthesis of Ligand (R_p)-7. During the time period of our work detailed above, Clayden and Arnott reported a method of reversing the preferred sense of

DOI: 10.1021/acs.joc.5b01766
J. Org. Chem. 2015, 80, 10163−10176

diastereoselectivity in ferrocene oxazoline directed *ortho*-lithiations.[21] This was accomplished using tridentate chelating agent **14** in place of TMEDA to provide the other diastereomer in 75% de (Scheme 3).

Scheme 3. Access to Both Diastereomers of Ferrocene *i*-Pr Oxazoline Using Different Chelating Agents[21]

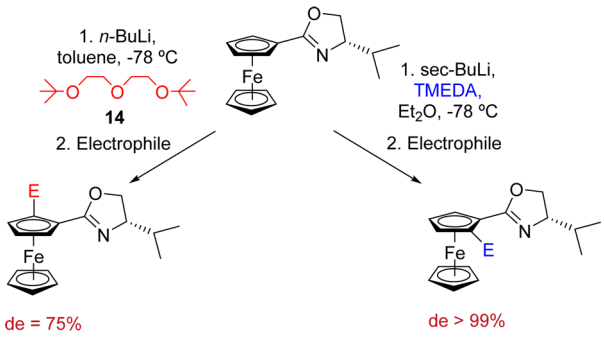

We sought to apply this to our own work in order to shorten the synthetic sequence of ligand (R_p)-**7** to just two steps from ferrocene oxazoline **8**. In the original synthesis of chelating agent **14**, the ditosylated intermediate **15** was treated with sodium *tert*-butoxide to provide **14** in 28% yield.[21] We found that substituting sodium *tert*-butoxide for the more nucleophilic and less basic lithium *tert*-butoxide provided the chelating agent **14** in an improved yield of 64% (Scheme 4).

Scheme 4. Synthesis of Chelating Agent 14

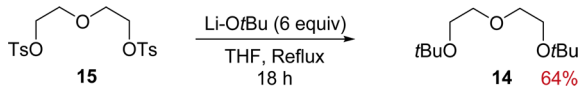

With chelating agent **14** in hand, we then carried out a directed *ortho*-lithiation on ferrocene oxazoline **8** utilizing the conditions described.[21] Unfortunately, only a modest de of 37.5% was obtained (Scheme 5). While the 37.5% de of **13**

Scheme 5. Lithiation of Ferrocene 8 with Chelating Agent 14

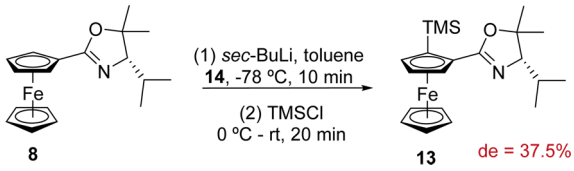

obtained may not be useful synthetically, it does provide a hint as to the conformation of the *i*-Pr group in our *gem*-dimethyl-substituted ligand precursor **8**.

Clayden and Arnott attempted diastereoselective lithiations of both *i*-Pr- and *t*-Bu-substituted ferrocene oxazolines and found that while the *i*-Pr oxazoline provided product with 75% de the *t*-Bu-substituted oxazoline yielded only a 1:1 diastereomeric mixture.[21] Thus, comparing the de values hints that the *i*-Pr group of our ferrocene oxazoline **8** has adopted a conformation halfway between that of an *i*-Pr group and a *t*-Bu group.

Ferrocene Oxazoline Lithiation Studies. During the course of our research, we sought to examine the lithiation complex formed upon deprotonation of ferrocene oxazoline **8** by an organolithium reagent. A nitrogen coordination mechanism has been postulated, and Sammakia has conducted studies in this area by synthesizing a tethered ferrocene oxazoline and subjecting this to lithiation.[22] The product obtained from this reaction indicates a lithium−nitrogen coordinated intermediate. Furthermore, Sebesta recently reported a computational study on the lithiation of ferrocene oxazolines via a nitrogen coordination pathway and showed that for ferrocene *i*-Pr-oxazoline with TMEDA the R_p lithiation transition state is more stable than the S_p by 19 kJ mol^{-1} due to steric interactions between the TMEDA−lithium chelate complex and the *i*-Pr group.[23] However, despite the many publications utilizing ferrocene oxazolines and DOM, such an N-coordinated lithiation intermediate has not been isolated. Therefore, we attempted to isolate and crystallize our lithiated ferrocene intermediate by cooling the lithiated reaction mix to −78 °C for 3 days in various solvent mixtures.[24] We proposed that a solvated dimer such as **16** would be formed upon deprotonation and thus hoped to isolate and crystallize this lithiated intermediate (Scheme 6).

Scheme 6. Lithiation and Attempted Crystallization of Ferrocene Oxazoline 8[a]

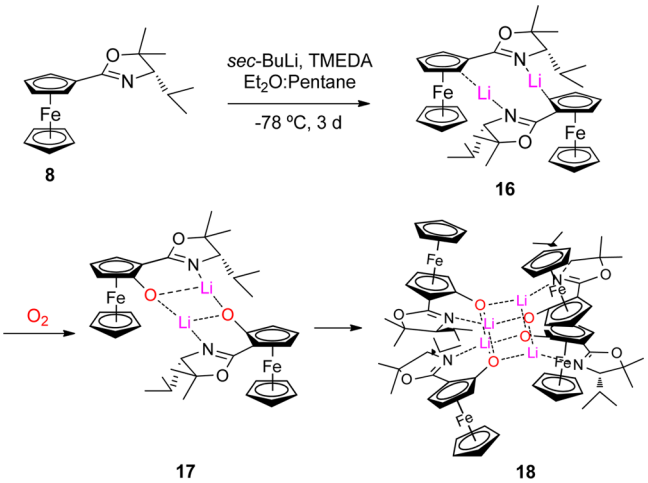

[a]Solvent atoms omitted for clarity.

After numerous attempts under various conditions, this approach proved unsuccessful. However, after adventitious exposure of the reaction mixture to air, crystallization occurred rapidly, providing crystals as small red blocks. X-ray analysis of these crystals provided the structure **18** shown in Scheme 6 and Figure 5.

This is a tetramer of an oxidized form of the proposed lithiation intermediate. We postulate that dimer **17** may have formed upon addition of molecular oxygen to the proposed lithiated intermediate **16** (Scheme 6). The oxidized intermediate **17** can then dimerize and crystallize as the tetrameric oxygen-containing species **18** (Scheme 6, Figure 5). Despite the fact that this is an oxidized intermediate of what we hoped to isolate, this is still the first example of any ferrocene oxazoline showing lithium−nitrogen coordination in the solid state. It should be noted that the sense of preferred diastereoselection observed experimentally is in place for each ferrocene in this structure. This structure adds further weight that the proposed lithium−nitrogen coordination mechanism

DOI: 10.1021/acs.joc.5b01766
J. Org. Chem. 2015, 80, 10163−10176

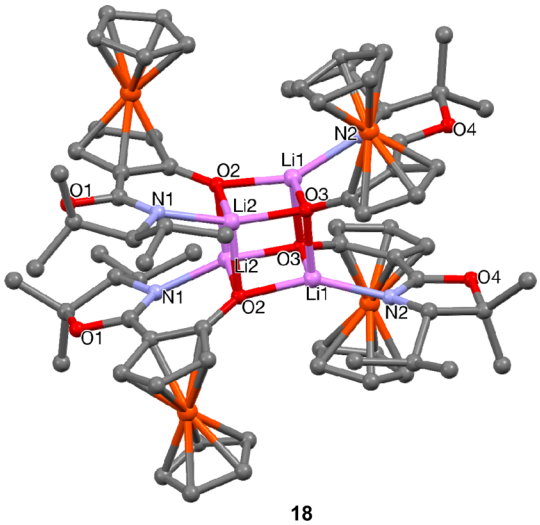

Figure 5. X-ray crystal structure of oxidized lithiation intermediate **18**.

is correct, supporting both Sammakia's lithiation studies and Sebesta's computational work. Upon addition of water, the monomeric hydrolysis product of **18** could be detected by ^{1}H NMR spectroscopy but unfortunately undergoes rapid decomposition and could not be isolated.

Diethylzinc Additions to Aldehydes. As both the *i*-Pr[16] (R_p)-**5** and *t*-Bu[15,25] (R_p)- and (S_p)-**4** derivatives of the ferrocenyl hydroxyoxazoline ligands have been applied in the dialkylzinc addition to aldehydes, we chose this as a suitable model reaction to evaluate our ligand class. This reaction has been extensively studied and so is an excellent testing ground for new concepts in ligand design.[26,27] Ligand (R_p)-**6** was applied to diethylzinc additions utilizing benzaldehyde as a model substrate in order to find optimal reaction conditions. Hexane provided superior ee's to toluene and was chosen as a suitable solvent, while lower temperatures of up to −20 °C proved optimal (Scheme 7, Table 1). It is noteworthy that

Scheme 7

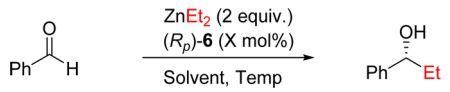

Table 1. Diethylzinc Additions to Benzaldehyde Catalyzed by Ligand (R_p)-6[a]

entry	solvent	temp (°C)	(R_p)-**6** (mol %)	time (h)	yield (%)	ee[b] (%)
1	toluene	0	10	4	96	80
2	toluene	−20	10	4	94	83
3	hexane	0	10	4	95	83
4	hexane	−20	10	5	90	87
5	hexane[c]	−20	10	5	95	87
6	hexane	−20	5	24	93	88
7	hexane	−40	5	24	69	88

[a]All reactions carried out on a 1 mmol scale. [b]Determined by HPLC analysis using a Chiralcel OD column. [c]3 equiv of diethylzinc was used. Configuration assigned by comparison with literature retention times.[25]

toluene was the optimal solvent for the *t*-Bu-analogue (R_p)-**4**, whereas the use of hexane led to reduced levels of enantioselectivity.[25] Applying 5 mol % of ligand (R_p)-**6**, using hexane as solvent at −20 °C, provided (*R*)-1-phenyl-1-propanol with 88% ee (Table 1, entry 6; Scheme 7).

We next investigated the performance of the remaining ferrocene ligands (S_p)-**6**, (R_p)-**7**, and (S_p)-**7** in the transformation using our optimized reaction conditions to determine the importance of planar chirality and the effect of an additional TMS group (Scheme 8).

From the results obtained, it is clear that planar chirality is the dominant factor controlling asymmetric induction with reversal of planar chirality between ligands (R_p)-**6** and (S_p)-**6** resulting in a 55% drop in ee with a coincident 61% drop in yield. It is noteworthy that both (R_p)-**6** and (S_p)-**6** provide results similar to those for the corresponding *t*-Bu ligands (R_p)-**4** and (S_p)-**4**, which provided product in 83% yield, 93% ee and 55% yield, 35% ee, respectively.[25] The additional TMS group present in ligands (R_p)-**7** and (S_p)-**7** has a pronounced effect on catalysis, lowering both ee and yield in the case of ligand (R_p)-**7** and providing nearly racemic product in the case of ligand (S_p)-**7**. We had initially hoped that the increased steric bulk provided by the TMS group would result in higher enantioselectivities; however, it appears the increased steric bulk is not beneficial. With these initial results we sought to further probe our ligand design. From consideration of our proposed transition states (*vide infra*) we wanted to investigate the effects of increased steric bulk beside the oxygen donor atom. From a brief literature survey, we found that this has previously resulted in increased ee's.[16,18] To examine this, we synthesized triferrocenyl ligand (R_p)-**19** in 64% yield via DOM of ferrocene oxazoline **8** and subsequent quench with diferrocenyl ketone (Scheme 9). Diferrocenyl ketone itself was synthesized in 90% yield via a modified literature procedure which originally yielded only 27%.[28]

Applying 5 mol % of ligand (R_p)-**19** using toluene as solvent at 40 °C provided (*R*)-1-phenyl-1-propanol in 79% yield with 93% ee after 7 h (optimized conditions, Table 2). The ee of 93% is an improvement upon the 88% ee from ligand (R_p)-**6** and matches the ee of Bolm's *t*-Bu FcOx (R_p)-**4** for benzaldehyde.[25] With both optimal ligands (R_p)-**6** and (R_p)-**19** in hand, a variety of other aldehydes were tested in order to examine the substrate scope (Table 2, Scheme 10).

Comparing these results with those obtained from the corresponding *t*-Bu (R_p)-**4** and *i*-Pr FcOx (R_p)-**5** analogues provides insight into how effective the *gem*-dimethyl *i*-Pr unit is at mimicking a *t*-Bu substituent.[15,16,25] With benzaldehyde and *p*-anisaldehyde, our *gem*-dimethyl based ligand (R_p)-**6** provides ee's almost exactly in between those provided by the *i*-Pr and *t*-Bu analogues (R_p)-**5** and (R_p)-**4**. With 4-chlorobenzaldehyde, no significant changes in ee were noted, while for *trans*-cinnamaldehyde the results are closer to those of the *i*-Pr analogue (R_p)-**5**. With ferrocene carboxaldehyde, the ee from our *gem*-dimethyl ligand (R_p)-**6** is nearly identical to that of the *t*-Bu-based ligand (R_p)-**4**. From these results, it is clear that the conformation of ligand (R_p)-**6**'s *i*-Pr group is different from those of both the *i*-Pr and *t*-Bu analogues (R_p)-**5** and (R_p)-**4**. This information corresponds with previous lithiation studies, where the diastereoselectivity upon lithiation of our *gem*-dimethyl ligand fell exactly halfway between those observed for the corresponding *i*-Pr and *t*-Bu analogues (vide supra, Scheme 5). Triferrocenyl ligand (R_p)-**19** provides higher ee's than ligand (R_p)-**6** and effectively mimics Bolm's *t*-Bu analogue

DOI: 10.1021/acs.joc.5b01766
J. Org. Chem. 2015, 80, 10163−10176

Scheme 8. Diethylzinc Addition to Benzaldehyde Catalyzed by Ligands 6 and 7[a]

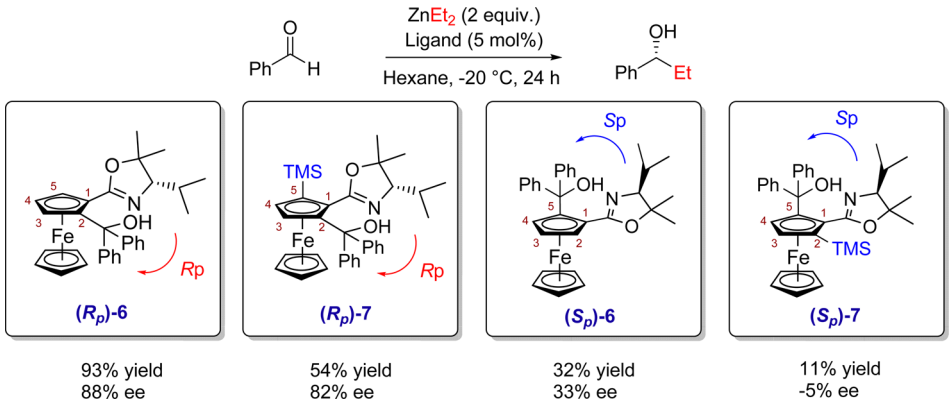

[a]All reactions carried out on a 1 mmol scale. Ee's were determined by HPLC using a Chiralcel OD column.

Scheme 9. Synthesis of Ligand (R_p)-19 via DOM of 8

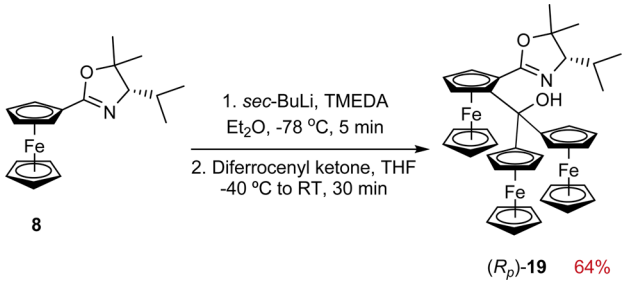

Scheme 10. Diethylzinc Addition to Aldehydes

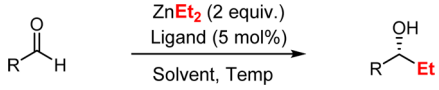

(R_p)-**4** for benzaldehyde, *p*-anisaldehyde, and *trans*-cinnamaldehyde while offering a significant improvement in enantioselectivity for 4-chlorobenzaldehyde. For ferrocene carboxaldehyde, the sterically congested ligand (R_p)-**19** provides slightly lower ee's than both ligand (R_p)-**6** and the *t*-Bu analogue (R_p)-**4**. Prompted by these results, we also wanted to examine our ligands performance with an *ortho*-substituted aldehyde and an aliphatic aldehyde, both of which generally provide lower levels of enantioselectivity.[18,26,27] With 1-naphthaldehyde, ligand (R_p)-**6** provided product in 81% ee, while ligand (R_p)-**19** gave 91% ee showing that high levels of enantioselectivity were possible with *ortho*-substituted aldehydes. With cyclohexane carboxaldehyde, ligand (R_p)-**6** provided an impressive ee of 96%, while ligand (R_p)-**19** furnished product with only 38% ee. The high ee obtained with cyclohexane carboxaldehyde is noteworthy, as in most cases aliphatic aldehydes provide much lower ee's than aromatic aldehydes.

Diphenylzinc Addition to Aldehydes. Encouraged by these results and wanting to further examine our ligands' performance, we decided to employ our ligand class in the more challenging phenylzinc addition to aldehydes.[18,29−32] This transformation facilitates the asymmetric synthesis of diarylmethanols, the main alternative to which is asymmetric reduction of diaryl ketones; however, this reduction methodology is highly substrate dependent.[33] Bolm and co-workers reported that using a mixed ethylphenylzinc reagent formed in situ from diethyl- and diphenylzinc resulted in selective phenyl transfer and provided increased ee's compared with diphenylzinc alone.[29] With this in mind, ligand (R_p)-**6** was applied in several phenyl additions utilizing 4-chlorobenzalde-

Table 2. Diethylzinc Addition to Various Aldehydes Catalyzed by Ligands (R_p)-6 and (R_p)-19[a]

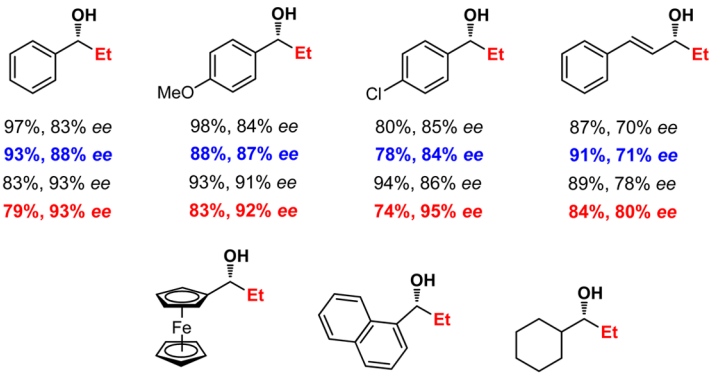

[16](R_p)-**5**	97%, 83% *ee*	98%, 84% *ee*	80%, 85% *ee*	87%, 70% *ee*
(R_p)-**6**	**93%, 88% *ee***	**88%, 87% *ee***	**78%, 84% *ee***	**91%, 71% *ee***
[15,25](R_p)-**4**	83%, 93% *ee*	93%, 91% *ee*	94%, 86% *ee*	89%, 78% *ee*
(R_p)-**19**	**79%, 93% *ee***	**83%, 92% *ee***	**74%, 95% *ee***	**84%, 80% *ee***

(R_p)-**6**	**92%, 93% *ee***	**79%, 81% *ee***	**72%, 96% *ee***
[15,25](R_p)-**4**	93%, 95% *ee*		
(R_p)-**19**	**93%, 91% *ee***	**74%, 91% *ee***	**86%, 38% *ee***

[a](R_p)-**6** conditions, hexane, −20 °C. (R_p)-**19** conditions, toluene, 40 °C. Ee's were determined by chiral HPLC or SFC, configuration determined by comparison with HPLC literature values, or tentatively assigned by assumption of an identical reaction pathway.

DOI: 10.1021/acs.joc.5b01766
J. Org. Chem. 2015, 80, 10163−10176

hyde as a model substrate in order to find optimal reaction conditions (Table 3, Scheme 11).

Table 3. Phenyl Addition to 4-Chlorobenzaldehyde Catalyzed by Ligand (R_p)-6[a]

entry	temp (°C)	ligand (mol %)	Ph_2Zn/Et_2Zn (equiv)	yield (%)	ee[b] (%)
1	10	5	1.5/0	83	72
2	10	5	0.65/1.3	82	92
3	10	10	0.65/1.3	88	92
4	rt[c]	5	0.65/1.3	89	91

[a]All reactions carried out on a 0.2 mmol scale for 24 h. [b]Determined by SFC using a Chiralpak IB column. [c]Room temperature was ~18 °C. Configuration determined by comparison of the optical rotation with literature value.[34]

Scheme 11. Phenyl Addition to 4-Chlorobenzaldehyde Catalyzed by Ligand (R_p)-6

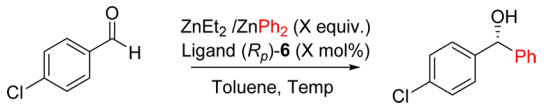

Optimal conditions were found by applying 5 mol % of ligand (R_p)-**6** with a mixed ethylphenylzinc reagent using toluene as solvent at 10 °C, providing 1-(4′-chlorophenyl)-1-propanol in 82% yield with 92% ee (Table 3, entry 2). We next investigated the performance of the remaining ferrocene ligands (S_p)-**6**, (R_p)-**7**, (S_p)-**7** and (R_p)-**19** using our optimized reaction conditions to determine the effect of changing planar chirality and the presence of an additional TMS group (Scheme 12).

As with the ethylzinc addition, it is clear that planar chirality is the dominant factor controlling asymmetric induction with reversal of planar chirality between ligands (R_p)-**6** and (S_p)-**6** reversing the stereochemical outcome of the reaction. This is particularly interesting as in the diethylzinc addition to aldehydes reversal of the ligands planar chirality did not reverse the stereochemical outcome but merely lowered the yield and ee. In terms of comparison, ligand (R_p)-**6** yields results similar to those of the corresponding *t*-Bu ligand (R_p)-**4**, which provided product in 92% yield with 95% ee under the same conditions.[29] Unfortunately, ligand (S_p)-**6**'s *t*-Bu analogue (S_p)-**4** was not tested, and thus, a direct comparison cannot be made. The additional TMS group present in ligands (R_p)-**7** and (S_p)-**7** has a pronounced effect on catalysis, lowering both ee's and yield's compared to their disubstituted counterparts (R_p)-**6** and (S_p)-**6**. Similar to the diethylzinc addition, it appears that the increased steric bulk from the TMS group is in fact detrimental. Bulky triferrocenyl ligand (R_p)-**19** provides an unusual result, forming product in 93% yield but with no enantioinduction. However, this is in agreement with another triferrocenyl system prepared by Butenschön and tested by Bolm.[16] We next tested a variety of other aldehydes in the ethylphenylzinc addition with optimal ligand (R_p)-**6** in order to examine the substrate scope (Table 4, Scheme 13).

Again, we will compare our results for ligand (R_p)-**6** with those obtained from the corresponding *t*-Bu analogue (R_p)-**4** to provide insight into how effective the *gem*-dimethyl *i*-Pr group is at mimicking the *t*-Bu substituent (Table 4).[29] For *p*-anisaldehyde, *p*-tolualdehyde, 4-chlorobenzaldehyde, and *trans*-cinnamaldehyde, ligand (R_p)-**6** provides results very similar to those of its *t*-Bu analogue (R_p)-**4**. With *ortho*-substituted 2-bromobenzaldehyde, ligand (R_p)-**6** provides a lower ee than its *t*-Bu counterpart (R_p)-**4** (82% vs 91%). However, with 1-naphthaldehyde, ligand (R_p)-**6** provides product in 90% ee, showing that high levels of enantioselectivity are possible with some *ortho*-substituted aldehydes. With ferrocene carboxaldehyde and cyclohexane carboxaldehyde, which gave the best results in the diethylzinc addition, we obtained excellent ee's of >99% and 99%, respectively.

X-ray Crystal Structures. To enable a better understanding of our results and to fully examine the impact of *gem*-disubstitution, we attempted to obtain the solid-state structures of all of our ligands. However, despite numerous attempts, a single crystal of (R_p)-**7** suitable for X-ray analysis could not be obtained. The crystal structures of ligands (R_p)-**6**, (S_p)-**6**, (S_p)-**7**, and (R_p)-**19** are shown in Figure 6.

In all structures we observe a seven membered chelate ring with the hydroxy proton strongly coordinated to the oxazoline nitrogen as expected. A detailed analysis of ligand (R_p)-**6** was deemed important as solid-state structures of both the *i*-Pr and *t*-Bu analogues (R_p)-**5** and (R_p)-**4** have been reported.[16,25] By comparing the three structures it is clear that the *i*-Pr

Scheme 12. Phenyl Addition to 4-Chlorobenzaldehyde Catalyzed by Ligands 6 and 7[a]

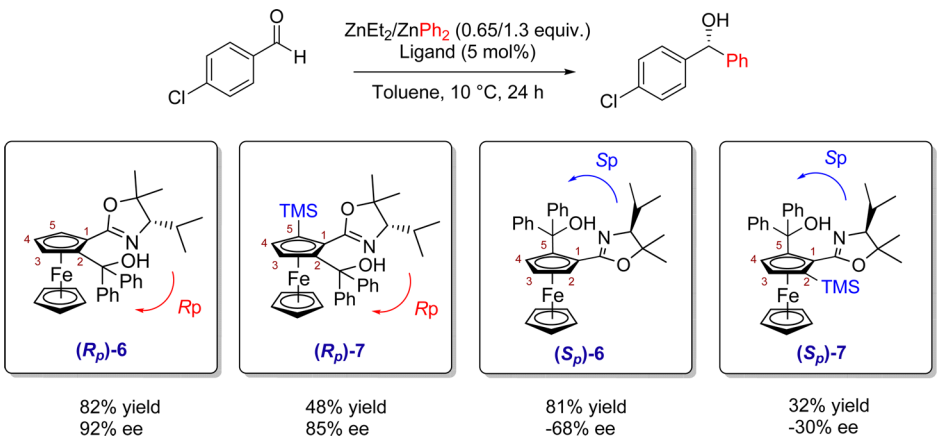

[a]All reactions carried out on a 0.2 mmol scale. Ee's were determined by SFC using a Chiralpak IB column.

DOI: 10.1021/acs.joc.5b01766
J. Org. Chem. 2015, 80, 10163−10176

Table 4. Phenyl Addition to Various Aldehydes Catalyzed by Ligand (R_p)-6[a]

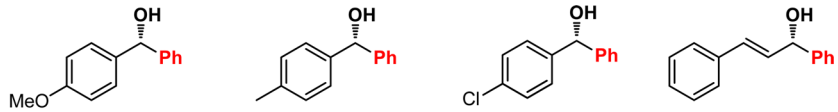

(R_p)-**6**	**80%, 94% *ee***	**72%, 93% *ee***	**78%, 92% *ee***	**65%, 87% *ee***
[29](R_p)-**4**	82%, 98% *ee*	86%, 98% *ee*	86%, 97% *ee*	97%, 90% *ee*

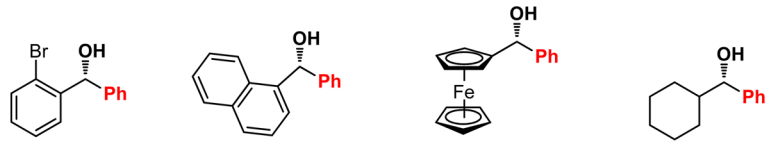

(R_p)-**6**	**68%, 82% *ee***	**77%, 90% *ee***	**79%, >99% *ee***	**53%, 99% *ee***
[29](R_p)-**4**	64%, 91% *ee*			

[a]Ee's were determined by chiral HPLC or SFC, configuration determined by comparison with HPLC literature values, or tentatively assigned by assumption of an identical reaction pathway.

Scheme 13. Phenyl Addition to Aldehydes Catalyzed by Ligand (R_p)-6

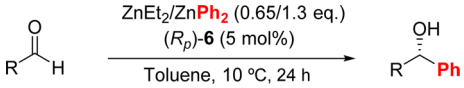

group in ligand (R_p)-**6** has adopted a solid-state conformation in-between that of an *i*-Pr and a *t*-Bu with the slight distortion of the oxazoline ring forcing the *i*-Pr group slightly closer to the metal center (Figure 7).

This conformation is closer to that of an *i*-Pr than a *t*-Bu group but whether this is dominant in solution is unknown. A similar motif is present in ligands (S_p)-**6** and (R_p)-**19** with both solid-state structures possessing a slightly distorted oxazoline ring and *i*-Pr group. In ligand (S_p)-**7** the introduction of an additional TMS group had a dramatic effect on the conformation of the *i*-Pr group compared to the corresponding disubstituted ligand (S_p)-**6**. The oxazoline ring has distorted only slightly but this minor distortion has resulted in the *i*-Pr group adopting a conformation similar to that of a *t*-Bu group, with the *i*-Pr group facing directly into

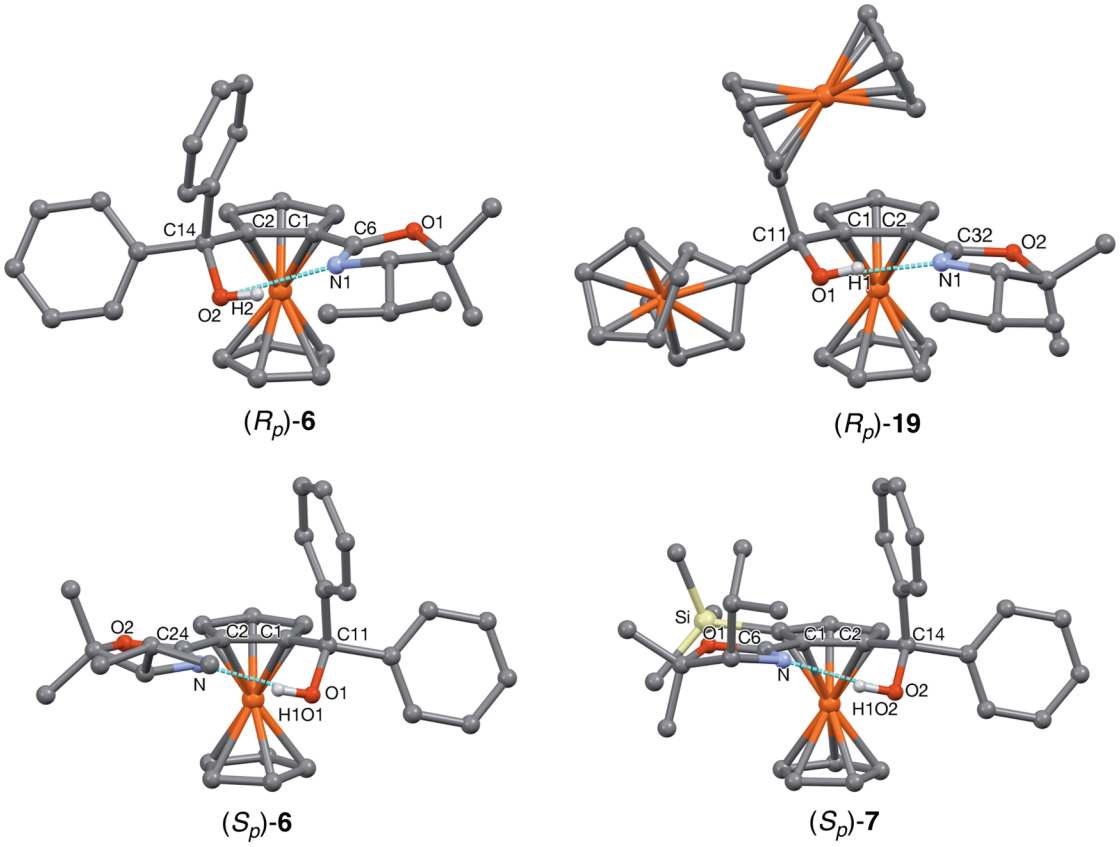

Figure 6. X-ray crystal structures of ligand (R_p)-**6** (top left), ligand (R_p)-**19** (top right), ligand (S_p)-**6** (bottom left), and ligand (S_p)-**7** (bottom right).

DOI: 10.1021/acs.joc.5b01766
J. Org. Chem. 2015, 80, 10163−10176

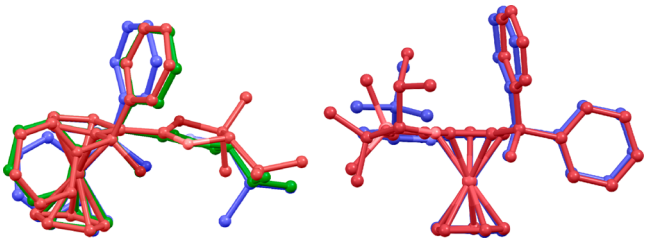

Figure 7. Overlay of crystal structures showing distortion of the oxazoline ring and rotation of the *i*-Pr group in ligand (R_p)-**6** (left) and ligand (S_p)-**7** (right). Order: (R_p)-**4** (blue, bottom),[25] (R_p)-**5** (green, middle),[16] (R_p)-**6** (left) or (S_p)-**7** (right) (red, top).

the axial phenyl group (Figure 7). This is noteworthy as it shows how a small change in the conformation of the oxazoline ring can result in the *i*-Pr group adopting a dramatically different conformation. It is possible that in solution the ligands adopt conformations similar to this, rather than those observed in the solid state, which would explain why the enantiomeric excesses obtained by ligand (R_p)-**6** are so similar to those induced by the *t*-Bu ligand (R_p)-**4**. However, from preliminary 2D NOESY experiments no interactions that could help elucidate the solution phase conformation of the oxazoline ring were found.

Transition States. Based on our X-ray crystal structures, we propose transition states similar to those proposed by previous investigators such as Noyori,[38] Norrby,[39] Corey,[40,41] and Houk[42] to rationalize the sense of asymmetric induction in the addition of ethyl and phenyl groups to aldehydes (Figure 8).

For ligands (R_p)-**6** and (R_p)-**19**, we propose *anti-cis* is the dominant transition state and the major source of the (*R*)-alcohol, while *syn-trans* is partially blocked due to steric repulsion between the ferrocene backbone and the aldehyde. All four *inv* transition states are blocked to some extent by the bulky aryl group on the top face of the alkoxide oxygen preventing *inv* coordination of the dialkylzinc, although when Ar = Ph, as in ligands **6** and **7**, this blocking may be imperfect. As *syn-cis* is completely blocked by the ferrocene backbone, this leaves the *anti-trans* transition state as a main source of (*S*)-alcohol. This helps explain why having a *t*-Bu group, rather than an *i*-Pr group, at C(4) of the oxazoline ring generally leads to higher ee's of (*R*)-alcohol. In this case, the steric repulsion between the C(4) group of the oxazoline and the R′ group of the aldehyde is the only inhibitor to this transition state. Thus, a bulkier group at C(4) will more successfully suppress this transition state and lead to increased ee's of the (*R*)-alcohol. These transition states also explain why ligand (R_p)-**19** provides better ee's than ligand (R_p)-**6**. The *inv* transition states leading to the (*S*)-alcohol are less hindered than those leading to the (*R*)-alcohol due to the position of the aldehyde's R′ group; thus, the *inv* transition states are likely an overall contributor to (*S*)-alcohol formation. However, in ligand (R_p)-**19** the bulky ferrocenyl groups will block the *inv* transition states much more effectively then the phenyl groups in ligand (R_p)-**6**, suppressing (*S*)-alcohol formation and resulting in increased ee's for ligand (R_p)-**19** (93% compared to 88% for ethyl transfer). For ligands (S_p)-**6** and (S_p)-**7** we propose similar transition states but with reversal of planar chirality on the ferrocene's Cp ring (Figure 9).

For the diethylzinc addition, ligand (S_p)-**6** provided (*R*)-alcohol in 33% ee; this can be explained by the mismatched blocking resulting from the *i*-Pr group now being *syn* to the axial phenyl group. Ideally, the blocking provided by the ferrocene backbone and the C(4) substituent on the oxazoline should be matched, as in the (R_p) ligands. For ligands (S_p)-**6** and (S_p)-**7** the *i*-Pr group and phenyl group block all of the *inv* transition states to some extent with the *inv* states leading to the (*S*)-alcohol encountering more steric hindrance due to the aldehyde's bulky R′ group facing the *i*-Pr group of the ligand. *Syn-cis* is completely blocked by the lower ferrocene ring, leaving the unhindered *anti-trans* as the major source of (*R*)-alcohol. *Anti-cis* is a minor source of (*S*)-alcohol with steric repulsion between the C(4) group of the oxazoline and the R′ group of the aldehyde suppressing this transition state. However, the major source of (*S*)-alcohol comes from *syn-trans,* which experiences only a small amount of steric repulsion between the lower ferrocene ring and the aldehydic

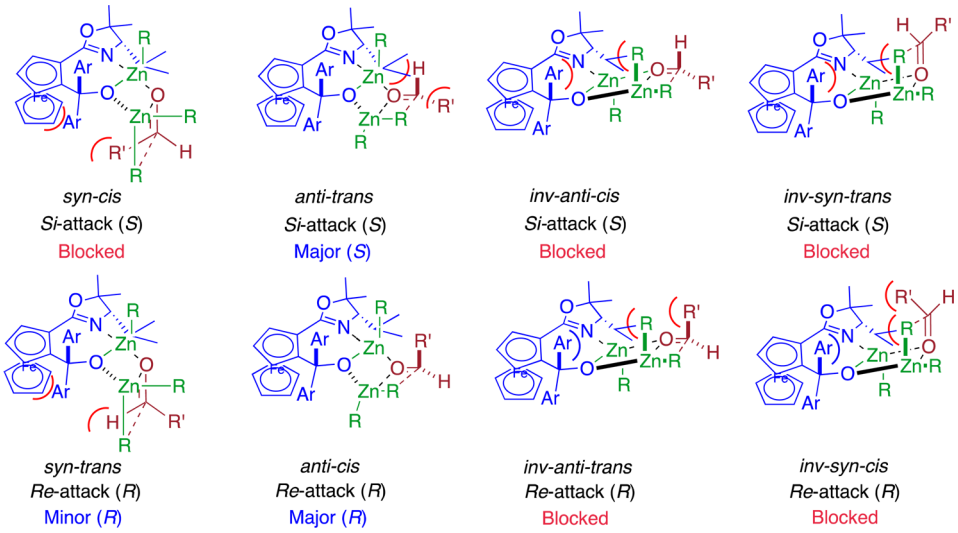

Figure 8. Possible transition states for the zinc alkoxides of our (R_p) chiral ligands (R_p)-**6**, (R_p)-**7**, and (R_p)-**19**. The terms *syn* and *anti* define the relationship between the transferring alkyl and the ferrocene backbone of the bidentate ligand. *Cis* and *trans* define which aldehyde lone-pair coordinates to the catalytic zinc chelated by the amino alcohol ligand. *Inv* implies inversion of configuration on the catalytic zinc.

DOI: 10.1021/acs.joc.5b01766
J. Org. Chem. 2015, 80, 10163−10176

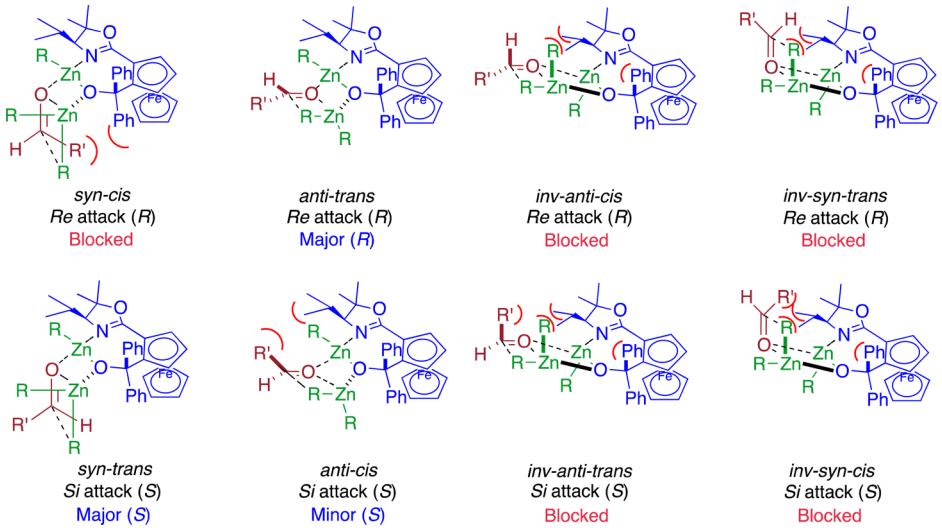

Figure 9. Possible transition states for the zinc alkoxides of our (S_p) chiral ligands (S_p)-**6** and (S_p)-**7**. The terms *syn* and *anti* define the relationship between the transferring alkyl and the ferrocene backbone of the bidentate ligand. C*is* and *trans* define which aldehyde lone pair coordinates to the catalytic zinc chelated by the amino alcohol ligand. *Inv* implies inversion of configuration on the catalytic zinc.

proton. Overall, this results in a small ee of the (*R*)-alcohol in the case of ligand (S_p)-**6** and nearly racemic product in the case of the more sterically congested ligand (S_p)-**7**.

The results from the mixed ethylphenylzinc addition are particularly interesting because in this reaction ligands (S_p)-**6** and (S_p)-**7** provided predominantly (*S*)-alcohol in good (68%) and moderate (30%) ee's, respectively (Scheme 12). This inversion of stereochemistry simply by changing the R group on the zinc is unprecedented. Based on previous studies, we assume a mixed ethylphenylzinc regent is formed and that the catalytic zinc is still bonded to an ethyl, rather than a phenyl group.[35−37] We postulate that this bulkier mixed reagent must destabilize the *anti-trans* conformation and suppress formation of the (*R*)-alcohol. Ligand (R_p)-**19** also behaves in a curious manner, providing excellent ee's in the diethylzinc addition but yielding only racemic product in the mixed ethylphenylzinc addition. From the crystal structure of ligand (R_p)-**19** we can see that the ferrocenyl group equatorial to the ligand backbone is pointing forward, directly into the space where the stoichiometric zinc needs to coordinate (Figure 6). We propose that when the bulkier ethylphenylzinc reagent is employed this undergoes steric interactions with the equatorial ferrocenyl group and leads to destabilization of the transition states hindering effective chiral induction.

Finally, we wanted to examine the effect of replacing the ferrocene backbone of our ligand with a simple phenyl ring. Previous reports indicate that this lowers ee's compared to the parent ferrocenyl backbone,[43] but Bolm and co-workers reported that this had little effect on their *t*-Bu FcOx ligand (R_p)-**4**.[25] This led to the design of ligand **20**, which is a phenyl-based derivative of ligands (R_p)-**6** and (S_p)-**6**. Not only would its use in catalysis provide insight into our transition states, but an X-ray crystal structure of such a ligand would be inherently interesting for comparative purposes. Ligand **20** was synthesized in an acceptable yield for testing purposes from the known *gem*-dimethyl precursor **21** via lithium/halogen exchange followed by quenching with benzophenone (Scheme 14).

Scheme 14. Synthesis of Ligand 20 via Lithium/Halogen Exchange of 21

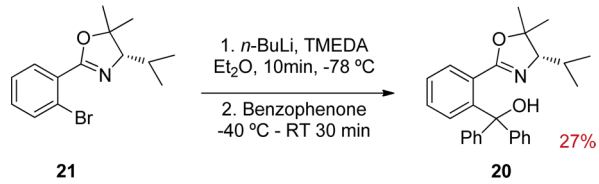

Application of ligand **20** in the diethylzinc addition to benzaldehyde under the same conditions as ligand (R_p)-**6** provided 1-phenyl-1-propanol in 83% yield but with only 67% ee. As the corresponding phenyl-*t*-Bu-oxazoline ligand provided product in 92% ee[25] this result was disappointing but did correlate with our transition states, which assign an important role to the ferrocene backbone in suppressing certain conformations (Figure 8). To provide further insight an X-ray crystal structure of ligand **20** was obtained (Figure 10).

From this structure, we can see that the *gem*-dimethyl effect is not apparent in the solid state; furthermore, the oxazoline ring is highly distorted. This is likely due to the more acute angle between the two substituents bonded to the phenyl ring compared to the Cp ring of ferrocene (123.51° between C14−C19−C20 in ligand **20** vs 127.16° between C2−C1−C6 in ligand (R_p)-**6**). This results in the nitrogen and oxygen donor atoms being closer together in **20**, which is disfavored due to the large size of the seven membered chelate ring. In order to accommodate this, the oxazoline ring distorts to provide some extra distance between the donor atoms resulting in the conformation we see in Figure 10.

■ CONCLUSIONS

We have reported the design, synthesis, and X-ray characterization of a total of six new ligands and their application in the ethyl and/or phenyl addition to both aromatic and aliphatic aldehydes providing secondary alcohols with excellent ee's of up to >99%. Application of the *gem*-dimethyl effect was successful, with our more economical ligands inducing similar levels of enantioselectivity to the correspond-

DOI: 10.1021/acs.joc.5b01766
J. Org. Chem. 2015, 80, 10163−10176

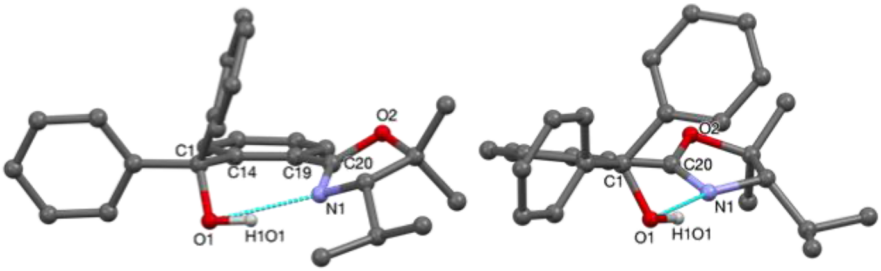

Figure 10. X-ray crystal structure of ligand **20**, front view (left) and side view (right).

ing expensive *t*-Bu ligands in the majority of cases. From our studies, we have determined that planar chirality is the dominant factor controlling asymmetric induction with reversal of planar chirality lowering ee's in the ethylzinc addition and reversing stereoselectivity in the phenylzinc addition. We have also demonstrated that trisubstituted ferrocene oxazoline ligands performed worse than their disubstituted counterparts in terms of both yield and ee. Furthermore, our lithiation studies yielded an interesting crystal structure of a ferrocenyl-oxide-lithium tetramer that shows for the first time, the proposed lithium−nitrogen coordination in the solid state. The excellent ee's of up to >99% obtained for phenyl addition to both aromatic and aliphatic aldehydes showcase our ligands as among the best available for these transformations while being readily synthesized from cheap starting materials.

■ EXPERIMENTAL SECTION

General Information. Unless otherwise noted, all commercial reagents were used as received without further purification. Anhydrous diethyl ether (Et_2O), tetrahydrofuran (THF), and dichloromethane (CH_2Cl_2) were obtained from a dry solvent dispenser. Aldehydes were purified by distillation, formation of the bisulfite derivative and regeneration with TMSCl, or simply by washing with 10% aqueous Na_2CO_3.[44,45]

General Procedure 1 (GP1) for Ferrocene Oxazoline Lithiation. Ferrocene oxazoline (1.0 equiv) was added to a dried, nitrogen-flushed Schlenk tube containing a magnetic stirring bar and dissolved in anhydrous Et_2O (2 mL/mmol). TMEDA (1.2 equiv) was added where required, and the reaction mixture was cooled to −78 °C before being treated dropwise with the appropriate organolithium reagent (1.1 equiv). After being stirred for 10 min at this temperature, the reaction was warmed to 0 °C and quenched with the electrophile (1.0 equiv). The resulting solution was allowed to warm to rt over 10−15 min before being quenched with saturated aqueous $NaHCO_3$, and the layers were separated. The organic extracts were washed with brine, dried ($MgSO_4$), filtered, and concentrated.

1-[(*S*)-4-Isopropyl-5,5-dimethyloxazolinyl]-2(S_p)-(trimethylsilyl)ferrocene (10). GP1 was followed utilizing ferrocene oxazoline **8** as the substrate on a 0.65 mmol scale, *s*-BuLi as the organolithium reagent, TMEDA as a chelating ligand, and TMSCl as the electrophile. Purification by column chromatography (pentane/EtOAc, 19:1) provided the disubstituted ferrocene oxazoline **10** (239.6 mg, 93%, one diastereomer by ^{1}H NMR) as a viscous red oil which solidified on standing: mp 92−94 °C (pentane); $[\alpha]^{20}_D$ = +89.4 (c = 1.00, $CHCl_3$); IR (film) ν_{max} 3108 (m), 2970 (m), 1655 (s), 1458 (m) cm^{-1}; ^{1}H NMR (400 MHz, $CDCl_3$) δ 4.92−4.86 (m, 1H), 4.46−4.37 (m, 1H), 4.27−4.21 (m, 1H), 4.18 (s, 5H), 3.26 (d, *J* = 8.6 Hz, 1H), 1.89−1.76 (m, 1H), 1.52 (s, 3H), 1.37 (s, 3H), 1.12 (d, *J* = 6.5 Hz, 3H), 0.99 (d, *J* = 6.5 Hz, 3H), 0.33 (s, 9H); ^{13}C{^{1}H} NMR (101 MHz, $CDCl_3$) δ 164.2, 85.9, 80.9, 77.0, 76.7, 73.2, 72.7, 71.6, 69.5, 29.27, 29.26, 21.6, 21.1*, 0.8 (*HSQC accounts for overlap of both Me carbons from the *i*-Pr group showing at 21.1); HRMS (ESI-TOF) calcd for $C_{21}H_{32}FeNOSi$ [M + H]$^+$ 398.1603, found 398.1620; TLC (pentane/EtOAc, 5:1) R_f 0.60 (UV, vis).

1-[(*S*)-4-Isopropyl-5,5-dimethyloxazolinyl]-2(S_p)-(trimethylsilyl)-5(S_p)-(diphenylmethanol)ferrocene ((S_p)-7). GP1 was followed utilizing ferrocene oxazoline **10** as the substrate on a 0.22 mmol scale, *n*-BuLi as the organolithium reagent, and benzophenone as the electrophile. Purification by column chromatography (pentane/EtOAc, 19:1) provided the trisubstituted ferrocene oxazoline (S_p)-7 (111.6 mg, 88% yield, 99% de) as a viscous red oil which solidified on standing. Recrystallization from pentane at rt led to the formation of red crystals that proved suitable for X-ray crystal analysis: mp 131−135 °C (pentane); $[\alpha]^{20}_D$ = +193.7 (*c* = 1.02, $CHCl_3$); IR (film) ν_{max} 3058 (m), 2960 (m), 2900−3100 (br), 1644 (s), 1411 (m) cm^{-1}; ^{1}H NMR (400 MHz, $CDCl_3$) δ 9.66 (s, 1H), 7.54−7.47 (m, 2H), 7.36−7.19 (m, 3H), 7.16−7.05 (m, 5H), 4.29 (s, 5H), 4.11 (d, *J* = 2.6 Hz, 1H), 3.71 (d, *J* = 2.5 Hz, 1H), 3.22 (d, *J* = 8.7 Hz, 1H), 1.46 (s, 3H), 1.20−1.06 (m, 1H), 0.81 (s, 3H), 0.75 (d, *J* = 5.1 Hz, 3H), 0.73 (d, *J* = 5.4 Hz, 3H), 0.30 (s, 9H); ^{13}C{^{1}H} NMR (101 MHz, $CDCl_3$) δ 167.1, 149.7, 147.0, 127.9, 127.7, 127.3, 127.2, 126.6, 126.3, 105.6, 87.9, 86.6, 79.9, 76.8, 74.3, 74.2, 72.4, 70.7, 29.0, 28.5, 20.9, 20.7, 20.7, 1.2; HRMS (ESI-TOF) calcd for $C_{34}H_{42}FeNO_2Si$ [M + H]$^+$ 580.2334, found 580.2347; TLC (pentane/EtOAc, 5:1) R_f 0.73 (UV, vis).

1-[(*S*)-4-Isopropyl-5,5-dimethyloxazolinyl]-2(S_p)-(diphenylmethanol)ferrocene ((S_p)-6). Ferrocene oxazoline ligand (S_p)-7 (288 mg, 0.477 mmol, 1.0 equiv) was added to a dry, nitrogen-flushed, 25 mL Schlenk tube equipped with a magnetic stirring bar and dissolved in 10 mL of THF. TBAF (5 mL, 1 M solution in THF, 10 equiv) was then added, and the resulting solution was heated to reflux with stirring for 72 h before being cooled to rt, partitioned with H_2O (10 mL), and separated before back extracting the H_2O with Et_2O (15 mL). Purification by column chromatography (pentane/Et_2O, 9:1) provided the disubstituted ferrocene oxazoline ligand (S_p)-**6** (199 mg, 79%, 99% de) as a viscous red oil which solidified on standing. Recrystallization from pentane at rt led to the formation of red crystals that proved suitable for X-ray crystal analysis: mp 123−124 °C (pentane); $[\alpha]^{20}_D$ = +225.6 (*c* = 1.25, $CHCl_3$); IR (film) ν_{max} 3087 (m), 2968 (m), 2921 (m), 3000 (br), 1644 (s), 1447 (m) cm^{-1}; ^{1}H NMR (400 MHz, $CDCl_3$) δ 9.49 (s, 1H), 7.55−7.48 (m, 2H), 7.35−7.18 (m, 3H), 7.17−7.00 (m, 5H), 4.71 (s, 1H), 4.27 (s, 5H), 4.21 (s, 1H), 3.67 (s, 1H), 3.32 (d, *J* = 6.1 Hz, 1H), 1.42 (s, 3H), 1.35−1.31 (m, 1H), 1.13 (s, 3H), 0.74 (d, *J* = 6.6 Hz, 3H), 0.31 (d, *J* = 6.5 Hz, 3H); ^{13}C{^{1}H} NMR (101 MHz, $CDCl_3$) δ 166.3, 149.5, 146.6, 127.9, 127.7, 127.3, 127.2, 126.6, 126.4, 101.1, 86.6, 79.2, 77.2, 74.9, 70.6, 70.2, 67.7, 67.1, 29.6, 28.8, 21.1, 21.0, 18.4; HRMS (ESI-TOF) calcd for $C_{31}H_{33}FeNO_2$ [M + Na]$^+$ 530.1758, found 530.1752; TLC (pentane/EtOAc, 5:1) R_f 0.85 (UV, vis).

1-[(*S*)-4-Isopropyl-5,5-dimethyloxazolinyl]-2(R_p)-(diphenylmethanol)ferrocene ((R_p)-6). GP1 was followed utilizing ferrocene oxazoline **8** as the substrate on a 2.32 mmol scale, *sec*-BuLi as the organolithium reagent, TMEDA as a chelating ligand, and benzophenone as the electrophile. Purification by column chromatography (pentane/Et_2O, 9:1) provided the disubstituted ferrocene oxazoline (R_p)-**6** (0.982 g, 83%, > 99% de) as a viscous red oil which solidified on standing. Recrystallization from pentane at rt led to the formation of red crystals that proved suitable for X-ray crystal

DOI: 10.1021/acs.joc.5b01766
J. Org. Chem. 2015, 80, 10163−10176

analysis: mp 127−130 °C (pentane); $[\alpha]^{20}_{D}$ = −197.4 (*c* = 0.98, $CHCl_3$); IR (film) ν_{max} 3085 (m), 2970 (m), 3000 (br), 1644 (s), 1447 (m) cm^{-1}; ^1H NMR (400 MHz, $CDCl_3$) δ 9.21 (s, 1H), 7.49−7.42 (m, 2H), 7.26−7.11 (m, 3H), 7.11−6.98 (m, 5H), 4.61 (s, 1H), 4.20 (s, 5H), 4.13 (s, 1H), 3.60 (s, 1H), 2.71 (d, *J* = 9.0 Hz, 1H), 1.79−1.65 (m, 1H), 1.25 (s, 3H), 1.19 (s, 3H), 1.01 (d, *J* = 6.5 Hz, 3H), 0.82 (d, *J* = 6.6 Hz, 3H); $^{13}C\{^1H\}$ NMR (101 MHz, $CDCl_3$) δ 166.0, 149.4, 146.4, 127.9, 127.5, 127.2, 127.1, 126.6, 126.2, 101.3, 86.7, 79.5, 77.3, 74.8, 70.7, 70.1, 67.7, 67.4, 28.9, 28.5, 21.5, 21.3, 20.8; HRMS (ESI-TOF) calcd for $C_{31}H_{34}FeNO_2$ $[M + H]^+$ 508.1939, found 508.1957; TLC (pentane/EtOAc, 5:1) R_f 0.82 (UV, vis).

1-[(*S*)-4-Isopropyl-5,5-dimethyloxazolinyl]-2(*R*$_p$)-iodo-5(*S*$_p$)-(trimethylsilyl)ferrocene (11). GP1 was followed utilizing ferrocene oxazoline **10** as the substrate on a 0.20 mmol scale and *n*-BuLi as the organolithium reagent. Freshly sublimed I_2 was used as the electrophile. No TMEDA was added. An additional wash with 10% aqueous $Na_2S_2O_3$ was performed to remove any remaining I_2. Purification by column chromatography (pentane/Et_2O, 9:1) provided the trisubstituted ferrocene oxazoline **11** (93.1 mg, 90%) as a viscous orange oil which quickly solidified on standing: mp 96−98 °C (pentane); $[\alpha]^{20}_{D}$ = +6.0 (*c* = 0.96, $CHCl_3$); IR (film) ν_{max} 3087 (m), 2924 (m), 1646 (s), 1422 (m), 1265 (m) cm^{-1}; ^1H NMR (400 MHz, $CDCl_3$) δ 4.67−4.61 (m, 1H), 4.24−4.22 (m, 1H), 4.21 (s, 5H), 3.30 (d, *J* = 9.8 Hz, 1H), 1.94−1.80 (m, 1H), 1.59 (s, 3H), 1.42 (s, 3H), 1.19 (d, *J* = 6.5 Hz, 3H), 0.99 (d, *J* = 6.4 Hz, 3H), 0.30 (s, 9H).; $^{13}C\{^1H\}$ NMR (101 MHz, $CDCl_3$) δ 162.2, 86.5, 81.6, 79.4, 77.4, 76.7, 73.2, 72.6, 44.4, 29.5, 29.1, 22.0, 21.8, 20.9, 0.5; HRMS (ESI-TOF) calcd for $C_{21}H_{31}IFeNOSi$ $[M + H]^+$ 524.0569, found 524.0563; TLC (pentane/Et_2O, 5:1.5) R_f 0.75 (UV, vis).

1-[(*S*)-4-Isopropyl-5,5-dimethyloxazolinyl]-2(*R*$_p$)-iodoferrocene (12). Trisubstituted ferrocene oxazoline **11** (0.423 g, 0.8 mmol, 1.0 equiv) was added to a 25 mL Schlenk tube equipped with a magnetic stirring bar and dissolved in 10 mL of THF. TBAF (2.0 mL, 1 M solution in THF, 2.5 equiv) was then added and the resulting solution heated to reflux with stirring overnight (16 h) before being cooled to rt, partitioned with H_2O (10 mL), and separated before back extracting the H_2O with Et_2O (15 mL). Purification by column chromatography (pentane/Et_2O, 9:1) provided the disubstituted ferrocene oxazoline **12** (354 mg, 97%, one diastereomer by ^1H NMR) as a viscous red oil: $[\alpha]^{20}_{D}$ = −28.7 (*c* = 0.47, $CHCl_3$); IR (film) ν_{max} 3099 (m), 2968 (m), 1655 (s), 1461 (m), 1246 (m) cm^{-1}; ^1H NMR (400 MHz, $CDCl_3$) δ 4.76−4.70 (m, 1H), 4.60−4.54 (m, 1H), 4.36−4.29 (m, 1H), 4.21 (s, 5H), 3.40 (d, *J* = 7.2 Hz, 1H), 1.90−1.78 (m, 1H), 1.50 (s, 3H), 1.43 (s, 3H), 1.10 (d, *J* = 6.5 Hz, 3H), 1.04 (d, *J* = 6.6 Hz, 3H); $^{13}C\{^1H\}$ NMR (101 MHz, $CDCl_3$) δ 162.6, 86.0, 80.0, 78.3, 73.3, 72.6, 70.9, 69.4, 39.7, 29.5, 29.4, 21.5, 21.4, 20.1; HRMS (ESI-TOF) calcd for $C_{18}H_{23}IFeNO$ $[M + H]^+$ 452.0174, found 452.0180; TLC (pentane/Et_2O, 5:1.5) R_f 0.25 (UV, vis).

1-[(*S*)-4-Isopropyl-5,5-dimethyloxazolinyl]-2(*R*$_p$)-(trimethylsilyl)ferrocene (13). GP1 was followed utilizing ferrocene oxazoline **12** as the substrate on a 0.64 mmol scale, *n*-BuLi as the organolithium reagent (1.0 equiv), and TMSCl as the electrophile. No TMEDA was added. Purification by column chromatography (pentane/Et_2O, 9:1) provided the disubstituted ferrocene trimethylsilyl oxazoline **13** (207 mg, 81%, one diastereomer by ^1H NMR) as a viscous red oil: $[\alpha]^{20}_{D}$ = −142.5 (c = 0.44, $CHCl_3$); IR (film) 3112 (m), 2966 (m), 1656 (s), 1241 (m) ν_{max} cm^{-1}; ^1H NMR (400 MHz, $CDCl_3$) δ 4.91−4.84 (m, 1H), 4.45−4.37 (m, 1H), 4.27−4.19 (m, 1H), 4.17 (s, 5H), 3.26 (d, *J* = 8.1 Hz, 1H), 1.87−1.74 (m, 1H), 1.49 (s, 3H), 1.35 (s, 3H), 1.11 (d, *J* = 6.5 Hz, 3H), 1.00 (d, *J* = 6.6 Hz, 3H), 0.31 (s, 9H); $^{13}C\{^1H\}$ NMR (101 MHz, $CDCl_3$) δ 163.8, 85.6, 80.7, 76.9, 76.6, 73.0, 73.0, 71.6, 69.5, 29.6, 29.2, 21.4, 21.3, 20.9, 0.7; HRMS (ESI-TOF) calcd for $C_{21}H_{31}FeNOSiNa$ $[M + Na]^+$ 420.1422, found 420.1418; TLC (pentane/Et_2O, 5:1.5) R_f 0.40 (UV, vis).

1-[(*S*)-4-Isopropyl-5,5-dimethyloxazolinyl]-2(*R*$_p$)-(diphenylmethanol)-5(*R*$_p$)-(trimethylsilyl)ferrocene ((*R*$_p$)-7). GP1 was followed utilizing ferrocene oxazoline **13** as the substrate on a 0.42 mmol scale, *n*-BuLi as the organolithium reagent, and benzophenone as the electrophile. Purification by column chromatography (pentane/Et_2O, 10:3) provided the trisubstituted ferrocene oxazoline (R_p)-**7** (196 mg, 80%, > 99% de) as a viscous red oil which solidified on standing: mp 88−92 °C (pentane); $[\alpha]^{20}_{D}$ = −233.9 (*c* = 0.75, $CHCl_3$); IR (film) ν_{max} 3086 (m), 2970 (m), 3000 (br), 1639 (s), 1412 (m) cm^{-1}; ^1H NMR (400 MHz, $CDCl_3$) δ 9.52 (s, 1H), 7.55−7.48 (m, 2H), 7.36−7.20 (m, 3H), 7.19−7.05 (m, 5H), 4.31 (s, 5H), 4.11 (d, *J* = 2.4 Hz, 1H), 3.71 (d, *J* = 2.5 Hz, 1H), 2.64 (d, *J* = 7.8 Hz, 1H), 1.82−1.69 (m, 1H), 1.32 (s, 3H), 1.06 (d, *J* = 6.5 Hz, 3H), 0.96 (s, 3H), 0.91 (d, *J* = 6.6 Hz, 3H), 0.30 (s, 9H); $^{13}C\{^1H\}$ NMR (101 MHz, $CDCl_3$) δ 166.7, 149.8, 146.9, 127.9, 127.5, 127.3, 127.2, 126.6, 126.2, 106.2, 86.6, 79.0, 77.4, 76.8, 76.7, 74.3, 74.0, 72.7, 70.7, 29.3, 28.9, 21.4, 21.3, 20.7, 1.1; HRMS (ESI-TOF) calcd for $C_{34}H_{41}FeNO_2Si$ $[M + H]^+$ 580.2334, found 580.2346. TLC (pentane/EtOAc, 5:1) R_f 0.70 (UV, vis).

Diferrocenyl Ketone. Synthesized via a modified literature procedure.[28] Oxalyl chloride (1.6 mL, 18.6 mmol, 3.3 equiv) was added under a nitrogen atmosphere with stirring to a solution of ferrocene carboxylic acid (1.30 g, 5.65 mmol, 1.0 equiv) in anhydrous CH_2Cl_2 (15 mL). The reaction was allowed to stir at rt for 1 h before removal of any remaining oxalyl chloride and solvent under vacuum leaving a dark red residue that was dried for a further 1 h. The crude ferrocene acid chloride was dissolved in CH_2Cl_2 (25 mL), and ferrocene (1.05 g, 5.65 mmol, 1.0 equiv) was added in one portion. The resulting solution was cooled (0 °C), and aluminum(III) chloride (0.75 g, 5.65 mmol, 1.0 equiv) was added in three portions over 15 min. The reaction was allowed to stir for 30 min with ice cooling before being refluxed for 1 h. The reaction was cooled again, and ice−water (50 mL) was slowly added. Stirring was continued for 5 min after which a biphasic mixture resulted. The layers were separated, and the aqueous layer was washed with CH_2Cl_2 (5 × 50 mL). The combined organic extracts were washed with 10% aqueous NaOH (2 × 50 mL) and brine (50 mL), dried with $MgSO_4$, and concentrated to give a crude red solid. Purification by column chromatography (pentane/CH_2Cl_2, 1:1) to remove unreacted ferrocene followed by (MeOH/CH_2Cl_2, 5:95) to speed up elution provided the title compound (2.02 g, 90%) as a red solid: mp 200−203 °C with dec (2-propanol) [lit.[28] 204 °C with decomposition (1-propanol)]; ^1H NMR (400 MHz, $CDCl_3$) δ 4.99 (s, 4H), 4.52 (s, 4H), 4.20 (s, 10H); $^{13}C\{^1H\}$ NMR (101 MHz, $CDCl_3$) δ 199.4, 80.6, 71.6, 70.8, 70.1; TLC (pentane/EtOAc, 5:1) R_f 0.71 (UV, vis). Matching known analytical data.[28]

1-[(*S*)-4-Isopropyl-5,5-dimethyloxazolinyl]-2-(*R*$_p$)-(diferrocenylmethanol)ferrocene ((*R*$_p$)-19). GP1 was followed utilizing ferrocene oxazoline **8** as the substrate on a 0.34 mmol scale and *s*-BuLi as the organolithium reagent. Diferrocenyl ketone was dissolved in 20 mL of THF before addition to the lithiated reaction mixture at −40 °C. The reaction mixture was allowed to stir for 30 min before quenching with aqueous saturated $NaHCO_3$. The product was dried using sodium sulfate as it is acid sensitive. Purification by column chromatography (pentane/CH_2Cl_2/EtOAc/TEA 70:20:5:5) provided the trisubstituted ferrocene oxazoline ligand (R_p)-**19** (196 mg, 80%, one diastereomer by ^1H NMR) as a viscous red oil which solidified on standing. Recrystallization from pentane/CH_2Cl_2 10:1 at rt led to the formation of red crystals that proved suitable for X-ray crystal analysis: mp 172−176 °C with dec (pentane/CH_2Cl_2, 10:1); $[\alpha]^{20}_{D}$ = +32.7 (*c* = 0.42, $CHCl_3$); IR (film) ν_{max} 3437 (m, br), 3100 (m), 2969 (m), 1653 (s), 1468 (m) cm^{-1}; ^1H NMR (400 MHz, $CDCl_3$) δ 8.96 (s, 1H), 4.76−4.61 (m, 3H), 4.27−4.08 (m, 6H), 4.06 (s, 5H), 4.05−4.02 (m, 1H), 4.01 (s, 5H), 3.96−3.91 (m, 1H), 3.87 (s, 5H), 3.44 (d, *J* = 9.0 Hz, 1H), 2.10−1.96 (m, 1H), 1.51 (s, 3H), 1.47 (s, 3H), 1.37 (d, *J* = 6.5 Hz, 3H), 1.09 (d, *J* = 6.6 Hz, 3H); $^{13}C\{^1H\}$ NMR (101 MHz, $CDCl_3$) δ 167.0, 101.5, 100.6, 99.9, 86.5, 80.7, 73.2, 72.3, 70.8, 70.3, 69.2, 68.7, 68.3, 68.3, 68.1, 67.9, 66.7, 66.6, 66.2, 66.1, 66.0, 65.9, 29.2, 29.1, 22.0, 21.7, 21.0; HRMS (ESI-TOF) calcd for $C_{39}H_{41}NO_2Fe_3$ $[M]^+$, 723.1185, found 723.1179. TLC (pentane/CH_2Cl_2/EtOAc/TEA, 70:20:5:5) R_f 0.75 (UV, vis).

DOI: 10.1021/acs.joc.5b01766
J. Org. Chem. 2015, 80, 10163−10176

(*S*)-(2-(4-Isopropyl-5,5-dimethyl-4,5-dihydrooxazol-2-yl)-phenyl)diphenylmethanol (20). GP1 was followed utilizing oxazoline **21** as the substrate on a 1.35 mmol scale with *n*-BuLi as the organolithium reagent and benzophenone as the electrophile. The product was dried using sodium sulfate as it is acid sensitive. Purification by column chromatography (CH_2Cl_2/acetone/TEA 80:20:1) to remove any excess benzophenone then (pentane/EtOAc/TEA 90:10:1) provided the trisubstituted oxazoline ligand **20** (146 mg, 27%) as a white, crystalline solid. Recrystallization from pentane/Et_2O 1:1 at rt led to the formation of clear, cubic crystals that proved suitable for X-ray crystal analysis: mp 142−145 °C (pentane/Et_2O, 1:1); $[\alpha]^{20}_D$ = −21.3 (*c* = 1.05, $CHCl_3$); IR (film) ν_{max} 3054 (m), 2977 (m), 2847−3091 (Br), 1649 (s), 1447 (m), 1265 (s) cm^{-1}; ^1H NMR (400 MHz, $CDCl_3$) δ 9.61 (s, 1H), 7.71 (dd, *J* = 7.6, 1.5 Hz, 1H), 7.50−7.14 (m, 12H), 6.71 (dd, *J* = 7.9, 1.2 Hz, 1H), 2.78 (d, *J* = 10.1 Hz, 1H), 1.61−1.47 (m, 1H), 1.23 (s, 3H), 1.10 (d, *J* = 6.5 Hz, 3H), 0.99 (s, 3H), 0.83 (d, *J* = 6.5 Hz, 3H); $^{13}C\{^1H\}$ NMR (101 MHz, $CDCl_3$) δ163.9, 148.7, 148.3, 147.2, 130.7, 130.4, 130.4, 128.1, 127.8, 127.8, 127.6, 127.3, 127.2, 126.8, 126.6, 87.0, 81.4, 80.3, 28.6, 28.4, 21.9, 20.8, 20.5; HRMS (ESI-TOF) calcd for $C_{27}H_{29}NO_2Na$ $[M + Na]^+$ 422.2096, found 422.2114; TLC (pentane/EtOAc 9:1) R_f 0.77 (UV).

Di-*tert*-butyl Diethylene Glycol (14). The compound was synthesized via a modified literature procedure.[21] A dry 500 mL round-bottom flask was placed under an inert atmosphere and charged with *t*-BuOH (60 mL, excess) and dry THF (40 mL). Lithium wire (1.5 g, 216 mmol, 6.0 equiv) was cut and rolled into thin small pieces before being added to the flask and stirred with a stirring bar. The flask was then refluxed for 4 h before being allowed to stir at rt overnight (16 h) after which ditosyl diglyme **15** (15.0 g, 36.0 mmol) was added and the flask brought to reflux for 18 h, followed by stirring at rt for a further 18 h. Pentane (100 mL) was added and the precipitate removed by filtration. The precipitate was washed with Et_2O (200 mL), the organic phases were combined, washed with satd aqueous $NaHCO_3$ solution (2 × 70 mL), and dried over $MgSO_4$, and the solvent was removed under reduced pressure. The resulting yellow oil was distilled (bulb-to-bulb) to provide a clear liquid (5.06 g, 23.2 mmol, 64%): bp 100 °C (ABT), 1 mbar; ^1H NMR (400 MHz, $CDCl_3$) δ 3.64−3.56 (m, 4H), 3.55−3.47 (m, 4H), 1.19 (s, 18H); $^{13}C\{^1H\}$ NMR (101 MHz, $CDCl_3$) δ 73.1, 71.4, 61.3, 27.7. Matching known analytical data.[21]

Chromatography of Ligands 6 and 7. Ligands **6** and **7** were analyzed via chiral SFC to determine accurate de values for the lithiation of ferrocene oxazoline **8**. As generating racemic material was difficult, we simply mixed a small amount of diastereomeric ligands (R_p)-**6** and (S_p)-**6** together and obtained a separation for this mixture. The same procedure was followed for the diastereomeric ligands (R_p)-**7** and (S_p)-**6**. SFC analysis of (R_p)-**6** and (S_p)-**6** (Chiralpak IC, CO_2/MeOH, 92:8), t_R = 2.96 min (R_p)-**6** and t_R = 3.80 min (S_p)-**6**. SFC analysis of (R_p)-**7** and (S_p)-**7** (Chiralpak IC, CO_2/2-propanol, 90:10), t_R = 1.99 min (R_p)-**7** and t_R = 2.75 min (S_p)-**7**.

General Procedure for Preparation of Racemic Alcohols. All racemic secondary alcohols were synthesized via Grignard addition of either EtMgBr or PhMgBr to the corresponding aldehyde in THF on a 3 mmol scale at rt.

General Procedure for the Diethylzinc Addition to Aldehydes (GP2). A well-dried Schlenk flask was charged with 5 mol % of the ligand precursor and cyclically flushed with nitrogen and evacuated three times. Anhydrous hexane (3 mL) was added and the solution cooled to −20 °C before addition of diethylzinc (1 M solution in hexane, 2 mL, 2 mmol, 2 equiv). The resulting solution was stirred for 20 min and the aldehyde (1.0 equiv) added. The reaction mixture was then sealed and monitored via TLC. Upon completion, 2 M HCl (5 mL) was added and the mixture stirred vigorously. The aqueous phase was extracted with CH_2Cl_2 (3 × 20 mL) and the combined organic phases washed with brine, dried ($MgSO_4$), filtered and concentrated before purification by column chromatography. For the studies utilizing 5 mol % of benzoic acid, this was added in directly after the aldehyde along with 1 mL of toluene to aid solubility.

In order to test our methodology we synthesized Bolm's *t*-Bu ferrocene oxazoline ligand (R_p)-**4** and carried out a test reaction utilizing Bolm's conditions for benzaldehyde. This provided 1-phenyl-1-propanol in 83% yield with 92% ee, nearly identical to the result obtained by Bolm (83% yield, 93% ee).[25]

1-Phenyl-1-propanol.[46] Purified by column chromatography (19:1 pentane/EtOAc) to give the product as a clear oil (107.9 mg, 79%, 93% ee): ^1H NMR (300 MHz, $CDCl_3$) δ 7.42−7.21 (m, 5H), 4.66−4.54 (m, 1H), 1.94−1.65 (m, 3H), 0.92 (t, *J* = 7.4 Hz, 3H); TLC (pentane/EtOAc, 5:1) R_f 0.45 (UV); HPLC analysis (Chiralcel OD, heptane/2-propanol = 98.5:1.5, 1 mL/min) t_R = 12.94 min (*R*) and t_R = 14.24 min (*S*).

1-(4′-Methoxyphenyl)-1-propanol.[46] Purified by column chromatography (19:1 pentane/EtOAc) to give the product as a clear oil (138.5 mg, 83%, 92% ee): ^1H NMR (300 MHz, $CDCl_3$) δ 7.27 (d, *J* = 8.4 Hz, 2H), 6.88 (d, *J* = 8.8 Hz, 2H), 4.55 (td, *J* = 6.6, 2.9 Hz, 1H), 3.81 (s, 3H), 1.99−1.63 (m, 3H), 0.90 (t, *J* = 7.4 Hz, 3H); TLC (pentane/EtOAc, 5:1) R_f 0.35 (UV); HPLC analysis (Chiralcel OD, heptane/2-propanol = 98.5:1.5, 1 mL/min) t_R = 18.18 min (*R*) and t_R = 20.73 min (*S*).

1-Cyclohexyl-1-propanol.[46] Purified by column chromatography (19:1 pentane/EtOAc) to give the product as a clear oil (102.7 mg, 72%, 96% ee). ^1H NMR (300 MHz, $CDCl_3$) δ 3.28 (dt, 1H), 1.88−0.99 (m, 14H), 0.95 (t, *J* = 7.4 Hz). TLC (pentane/EtOAc, 5:1) R_f 0.65 (Vanillin). The % ee of the benzoate derivative was determined by chiral HPLC. (Formed by reaction of 1-cyclohexyl-1-propanol with 1 equiv of benzoyl chloride in the presence of 1 equiv of triethylamine). HPLC analysis (Chiralcel OD, heptane/2-propanol = 99.5/0.5, 0.5 mL/min) t_R = 9.96 min (*R*) and t_R = 11.27 min (*S*).

(E)-1-Phenyl-1-penten-3-ol.[46] Purified by column chromatography (19:1 pentane/EtOAc) to give the product as a clear oil (136.3 mg, 84%, 80% ee): ^1H NMR (300 MHz, $CDCl_3$) δ 7.44−7.17 (m, 5H, H_{ar}), 6.58 (dd, *J* = 16.0, 1.3 Hz, 1H), 6.22 (dd, *J* = 15.9, 6.7 Hz, 1H), 4.28−4.15 (m, 1H), 1.77−1.54 (m, 2H), 0.98 (t, *J* = 7.4 Hz, 3H). TLC (pentane/EtOAc, 5:1) R_f 0.68 (UV): HPLC analysis (Chiralcel OD, heptane/2-propanol = 90/10, 1 mL/min) t_R = 6.43 min (*R*) and t_R = 8.60 min (*S*).

1-(1′-Naphthyl)-1-propanol.[46] Purified by column chromatography (19:1 pentane/EtOAc) to give the product as a clear oil (138.0 mg, 74%, 91% ee): ^1H NMR (300 MHz, $CDCl_3$) δ 8.18−8.07 (m, 1H), 7.92−7.83 (m, 1H), 7.78 (d, *J* = 8.2 Hz, 1H), 7.64 (d, *J* = 7.1 Hz, 1H), 7.58−7.42 (m, 3H), 5.42 (dt, *J* = 8.1, 4.4 Hz, 1H), 2.03−1.86 (m, 2H), 1.04 (t, *J* = 7.4 Hz, 3H); TLC (pentane/EtOAc, 5:1) R_f 0.47 (UV); HPLC analysis (Chiralcel OD, heptane/2-propanol = 95/5, 1 mL/min) t_R = 10.11 min (*S*) and t_R = 16.48 min (*R*).

1-(4′-Chlorophenyl)-1-propanol.[46] Purified by column chromatography (19:1 pentane/EtOAc) to give the product as a white solid (126.4 mg, 74%, 95% ee): TLC (pentane/EtOAc, 5:1) R_f 0.67 (UV). ^1H NMR (300 MHz, $CDCl_3$) δ 7.50−7.01 (m, 4H), 4.58 (t, *J* = 6.5 Hz, 1H), 1.97−1.50 (m, 3H), 0.90 (t, *J* = 7.4 Hz, 3H); HPLC analysis (Chiralpak AD, heptane/2-propanol = 99.5/0.5, 1 mL/min) t_R = 24.11 min (*S*) and t_R = 26.13 min (*R*).

Ferrocenyl-1-propanol.[46] Purified by column chromatography (19:1 pentane/EtOAc) to give the product as an orange solid (224.6 mg, 92%, 93% ee): TLC (pentane/EtOAc, 5:1) R_f 0.75 (UV). ^1H NMR (400 MHz, $CDCl_3$) δ 4.30−4.12 (m, 10H), 1.93 (d, *J* = 3.4 Hz, 1H), 1.76−1.60 (m, 2H), 0.94 (t, *J* = 7.4 Hz, 3H); SFC analysis (Chiralpak IC, CO_2/MeOH gradient as shown in Table 5) t_R = 2.77 min (*S*) and t_R = 2.84 min (*R*).

General Procedure for the Ethylphenylzinc Addition to Aldehydes (GP3). A well-dried Schlenk flask under an atmosphere of nitrogen was charged with diphenylzinc (28 mg, 0.13 mmol, 0.65 equiv) before being cyclically flushed with nitrogen and evacuated three times. Anhydrous toluene (3 mL) and diethylzinc (1 M solution in hexane, 0.26 mL, 0.26 mmol, 1.30 equiv) were added, and the solution was cooled to 10 °C and stirred for 30 min. The ligand precursor (5 mol %) was added and the resulting solution stirred for a further 20 min before addition of the aldehyde (0.20

DOI: 10.1021/acs.joc.5b01766
J. Org. Chem. 2015, 80, 10163−10176

Table 5. Chromatography Conditions for Analysis of Ferrocenyl-1-propanol

	time (min)	flow rate (mL/min)	% CO_2	% MeOH
1	initial	3.0	99.0	1.0
2	1.00	3.0	99.0	1.0
3	5.00	3.0	60.0	40.0
4	5.10	3.0	99.0	1.0

mmol, 1 equiv). The reaction mixture was sealed and monitored via TLC. Upon completion, 2 M HCl (5 mL) was added and the mixture stirred vigorously. The aqueous phase was extracted with CH_2Cl_2 (3 × 20 mL), and the combined organic phases were washed with brine, dried ($MgSO_4$), filtered, and concentrated before purification by column chromatography. For the studies utilizing 5 mol % of benzoic acid, this was added in directly after the aldehyde.

4-Chlorophenyl(phenyl)methanol.[47] Purified by column chromatography (19:1 pentane/EtOAc) to give the product as a white solid (34.3 mg, 78%, 92% ee): TLC (pentane/EtOAc, 5:1) R_f 0.60 (UV); ^{1}H NMR (300 MHz, $CDCl_3$) δ 7.39−7.21 (m, 9H), 5.83 (app d, J = 3.5 Hz, 1H), 2.18 (app d, J = 3.5 Hz, 1H). SFC analysis (Chiralpak IB, CO_2/MeOH = 94:6, 2 mL/min) t_R = 4.42 min (S) and t_R = 4.72 min (R).

4-Methoxyphenyl(phenyl)methanol.[47] Purified by column chromatography (19:1 pentane/EtOAc) to give the product as a clear oil which solidifies on standing to give a white solid (34.3 mg, 80%, 94% ee): TLC (pentane/EtOAc, 5:1) R_f 0.45 (UV); ^{1}H NMR (400 MHz, $CDCl_3$) δ 7.42−7.21 (m, 7H), 6.91−6.82 (m, 2H), 5.82 (d, J = 3.2 Hz, 1H), 3.79 (d, J = 0.7 Hz, 3H), 2.13 (d, J = 3.4 Hz, 1H). SFC analysis (Chiralpak IB, CO_2/MeOH = 94:6, 2 mL/min) t_R = 5.08 min (S) and t_R = 5.40 min (R).

(E)-1,3-Diphenylprop-2-en-1-ol.[48] Purified by column chromatography (19:1 pentane/EtOAc) to give the product as a clear, slightly yellow oil (27.4 mg, 65%, 87% ee): TLC (pentane/EtOAc, 5:1) R_f 0.53 (UV); ^{1}H NMR (400 MHz, $CDCl_3$) δ 7.48−7.19 (m, 10H), 6.70 (d, J = 15.8 Hz, 1H), 6.40 (dd, J = 15.8, 6.5 Hz, 1H), 5.40 (dd, J = 6.2, 3.6 Hz, 1H), 2.00 (d, J = 3.6 Hz, 1H). SFC analysis (Chiralpak IB, CO_2/MeOH = 94:6, 2 mL/min) t_R = 5.17 min (R) and t_R = 5.43 min (S).

Naphthalen-1-ylphenylmethanol.[48] Purified by column chromatography (19:1 pentane/EtOAc) to give the product as a clear oil (37.1 mg, 79%, 90% ee): TLC (pentane/EtOAc, 5:1) R_f 0.62 (UV); ^{1}H NMR (300 MHz, $CDCl_3$) δ 8.10−7.99 (m, 1H), 7.93−7.77 (m, 2H), 7.69−7.60 (m, 1H), 7.55−7.21 (m, 8H), 6.56 (d, J = 3.7 Hz, 1H), 2.32 (d, J = 4.0 Hz, 1H). SFC analysis (Chiralpak IB, CO_2/MeOH gradient as shown in Table 6) t_R = 3.69 min (S) and t_R = 4.23 min (R).

Table 6. Chromatography Conditions for Analysis of Naphthalen-1-yl(phenyl)methanol

	time (min)	flow rate (mL/min)	% CO_2	% MeOH
1	initial	3.0	99.0	1.0
2	1.00	3.0	99.0	1.0
3	5.00	3.0	60.0	40.0
4	5.10	3.0	99.0	1.0

p-Tolyl(phenyl)methanol.[47] Purified by column chromatography (19:1 pentane/EtOAc) to give the product as a clear oil which slowly solidifies to give a white solid (28.6 mg, 72%, 93% ee): TLC (pentane/EtOAc, 5:1) R_f 0.65 (UV); ^{1}H NMR (300 MHz, $CDCl_3$) δ 7.48−7.05 (m, 9H), 5.83 (d, J = 3.7 Hz, 1H), 2.33 (s, 3H), 2.13 (app d, J = 3.6 Hz, 1H). SFC analysis (Chiralpak IB, CO_2/MeOH = 94/6, 2 mL/min) t_R = 3.36 min (S) and t_R = 3.72 min (R).

2-Bromophenyl(phenyl)methanol.[47] Purified by column chromatography (19:1 pentane/EtOAc) to give the product as a viscous yellow oil (36.0 mg, 68%, 82% ee): TLC (pentane/EtOAc, 5:1) R_f 0.77 (UV); ^{1}H NMR (400 MHz, $CDCl_3$) δ 7.62−7.50 (m, 2H), 7.45−7.20 (m, 6H), 7.20−7.11 (m, 1H), 6.21 (d, J = 3.8 Hz, 1H), 2.34 (d, J = 3.8 Hz, 1H). HPLC analysis (Chiralcel OD, heptane/2-propanol = 99.5/0.5, 1 mL/min) t_R = 47.81 min (R) and t_R = 59.23 min (S).

Cyclohexyl(phenyl)methanol.[47] Purified by column chromatography (19:1 pentane/EtOAc) to give the product as a clear oil (20.2 mg, 53%, 99% ee): TLC (pentane/EtOAc, 5:1) R_f 0.75 (UV); ^{1}H NMR (400 MHz, $CDCl_3$) δ 7.39−7.20 (m, 5H), 4.37 (dd, J = 7.2, 3.2 Hz, 1H), 2.03−1.94 (m, 1H), 1.79 (d, J = 3.2 Hz, 1H), 1.78−1.55 (m, 3H), 1.43−1.32 (m, 1H), 1.31−0.86 (m, 6H). HPLC analysis (Chiralcel OD, heptane/2-propanol = 99.5/0.5, 0.5 mL/min) t_R = 41.62 min (S) and t_R = 44.81 min (R).

Ferrocenyl(phenyl)methanol.[48] Purified by column chromatography (19:1 pentane/EtOAc) to give the product as a red solid (46.2 mg, 79%, > 99% ee): TLC (pentane/EtOAc, 5:1) R_f 0.65 (UV); ^{1}H NMR (300 MHz, $CDCl_3$) δ 7.44−7.19 (m, 5H), 5.47 (app d, J = 3.1 Hz, 1H), 4.29−4.14 (m, 9H), 2.44 (app d, J = 3.2 Hz, 1H). SFC analysis (Chiralpak IC, CO_2/2-propanol gradient as shown in Table 7) t_R = 2.47 min (R) and t_R = 2.61 min (S).

Table 7. Chromatography Conditions for Analysis of Ferrocenyl(phenyl)methanol

	time (min)	flow rate (mL/min)	% CO_2	% 2-propanol
1	initial	3.0	99.0	1.0
2	1.00	3.0	99.0	1.0
3	5.00	3.0	60.0	40.0
4	5.10	3.0	99.0	1.0

■ ASSOCIATED CONTENT

Supporting Information

The Supporting Information is available free of charge on the ACS Publications website at DOI: 10.1021/acs.joc.5b01766. CCDC 1415501−1415506 contain the supplementary crystallographic data for this paper. This data can be obtained free of charge from the Cambridge Crystallographic Data Centre via www.ccdc.cam.ac.uk/data_request/cif.

X-ray data (CIF)
Full analysis for all new compounds including NMR, X-ray, and chromatographic data (PDF)

■ AUTHOR INFORMATION

Corresponding Author

* E-mail: p.guiry@ucd.ie

Notes

The authors declare no competing financial interest.

■ ACKNOWLEDGMENTS

We thank the Irish Research Council (IRC) for the award of a research scholarship (RS/2012/607) to C.N. We also thank the UCD School of Chemistry for the use of analytical facilities and the technical staff, Dr. Yannick Ortin and Geraldine Fitzpatrick for NMR spectroscopy and Adam Coburn and Kevin Conboy for mass spectrometry. Dr. Mike Casey is kindly acknowledged for a helpful discussion regarding the potential influence of benzoic acid.

■ REFERENCES

(1) Dawson, G. J.; Frost, C. G.; Williams, J. M. J.; Coote, S. J. *Tetrahedron Lett.* **1993**, *34*, 3149.
(2) Sprinz, J.; Helmchen, G. *Tetrahedron Lett.* **1993**, *34*, 1769.
(3) von Matt, P.; Pfaltz, A. *Angew. Chem., Int. Ed. Engl.* **1993**, *32*, 566.

DOI: 10.1021/acs.joc.5b01766
J. Org. Chem. 2015, 80, 10163−10176

(4) Hargaden, G. C.; Guiry, P. J. *Chem. Rev.* **2009**, *109*, 2505.
(5) McManus, H. A.; Guiry, P. J. *Chem. Rev.* **2004**, *104*, 4151.
(6) Desimoni, G.; Faita, G.; Jørgensen, K. A. *Chem. Rev.* **2006**, *106*, 3561.
(7) Desimoni, G.; Faita, G.; Jørgensen, K. A. *Chem. Rev.* **2011**, *111*, PR284.
(8) Carroll, M. P.; Guiry, P. J. *Chem. Soc. Rev.* **2014**, *43*, 819.
(9) (*S*)-*tert*-Leucine costs €36/g, and (*R*)-*tert*-leucine costs €366/g on sigmaaldrich.com (checked Jan 11, 2015).
(10) Belanger, E.; Pouliot, M. F.; Paquin, J. F. *Org. Lett.* **2009**, *11*, 2201.
(11) Bélanger, É.; Pouliot, M.-F.; Courtemanche, M.-A.; Paquin, J.-F. *J. Org. Chem.* **2012**, *77*, 317.
(12) McCartney, D.; Nottingham, C.; Müller-Bunz, H.; Guiry, P. J. *J. Org. Chem.* **2015**, DOI: 10.1021/acs.joc.5b01764.
(13) O' Reilly, S.; Aylward, M.; Keogh-Hansen, C.; Fitzpatrick, B.; McManus, H.; Müller-Bunz, H.; Guiry, P. J. *J. Org. Chem.* **2015**, DOI: 10.1021/acs.joc.5b01767.
(14) Craig, R. A., II; Stoltz, B. M. *Tetrahedron Lett.* **2015**, *56*, 4670.
(15) Bolm, C.; Fernandez, K. M.; Seger, A.; Raabe, G. *Synlett* **1997**, *9*, 1051.
(16) Garabatos-Perera, J. R.; Butenschön, H. *J. Organomet. Chem.* **2009**, *694*, 2047.
(17) Patti, A.; Nicolosi, G.; Howell, J. A. S.; Humphries, K. *Tetrahedron: Asymmetry* **1998**, *9*, 4381.
(18) Ahern, T.; Müller-Bunz, H.; Guiry, P. J. *J. Org. Chem.* **2006**, *71*, 7596.
(19) Sammakia, T.; Latham, H. A.; Schaad, D. R. *J. Org. Chem.* **1995**, *60*, 10.
(20) Conditions: (i) DIPEA, NaI, MOMCl, dimethoxyethane; (ii) DIPEA, MOMCl, dichloromethane; (iii) *s*-BuLi, TMSCl, diethyl ether.
(21) Herbert, S. A.; Castell, D. C.; Clayden, J.; Arnott, G. E. *Org. Lett.* **2013**, *15*, 3334.
(22) Sammakia, T.; Latham, H. A. *J. Org. Chem.* **1996**, *61*, 1629.
(23) Skvorcova, A.; Sebesta, R. *Org. Biomol. Chem.* **2014**, *12*, 132.
(24) Solvent systems used: diethyl ether/pentane = (1) 25:75, (2) 50:50, (3) 75:25, and (4) 50:50 with a small amount of THF added after lithiation in an attempt to induce crystallization.
(25) Bolm, C.; Muñiz-Fernández, K.; Seger, A.; Raabe, G.; Günther, K. *J. Org. Chem.* **1998**, *63*, 7860.
(26) Soai, K.; Niwa, S. *Chem. Rev.* **1992**, *92*, 833.
(27) Pu, L.; Yu, H.-B. *Chem. Rev.* **2001**, *101*, 757.
(28) Rausch, M. D.; Fischer, E. O.; Grubert, H. *J. Am. Chem. Soc.* **1960**, *82*, 76.
(29) Bolm, C.; Hermanns, N.; Hildebrand, J. P.; Muñiz, K. *Angew. Chem., Int. Ed.* **2000**, *39*, 3465.
(30) Bolm, C.; Muniz, K. *Chem. Commun.* **1999**, 1295.
(31) Bolm, C.; Rudolph, J. *J. Am. Chem. Soc.* **2002**, *124*, 14850.
(32) Kim, J. G.; Walsh, P. J. *Angew. Chem., Int. Ed.* **2006**, *45*, 4175.
(33) Ohkuma, T.; Koizumi, M.; Ikehira, H.; Yokozawa, T.; Noyori, R. *Org. Lett.* **2000**, *2*, 659.
(34) Qin, Y.-C.; Pu, L. *Angew. Chem., Int. Ed.* **2006**, *45*, 273.
(35) Fontes, M.; Verdaguer, X.; Solà, L.; Pericàs, M. A.; Riera, A. *J. Org. Chem.* **2004**, *69*, 2532.
(36) Rudolph, J.; Bolm, C.; Norrby, P.-O. *J. Am. Chem. Soc.* **2005**, *127*, 1548.
(37) Rudolph, J.; Rasmussen, T.; Bolm, C.; Norrby, P.-O. *Angew. Chem., Int. Ed.* **2003**, *42*, 3002.
(38) Yamakawa, M.; Noyori, R. *Organometallics* **1999**, *18*, 128.
(39) Rasmussen, T.; Norrby, P.-O. *J. Am. Chem. Soc.* **2003**, *125*, 5130.
(40) Corey, E. J.; Hannon, F. J. *Tetrahedron Lett.* **1987**, *28*, 5233.
(41) Corey, E. J.; Hannon, F. J. *Tetrahedron Lett.* **1987**, *28*, 5237.
(42) Goldfuss, B.; Houk, K. N. *J. Org. Chem.* **1998**, *63*, 8998.
(43) Stangeland, E. L.; Sammakia, T. *Tetrahedron* **1997**, *53*, 16503.
(44) Armarego, W. L.; Chai, C. *Purification of Laboratory Chemicals*; Butterworth-Heinemann: London, 2012.
(45) Kjell, D. P.; Slattery, B. J.; Semo, M. J. *J. Org. Chem.* **1999**, *64*, 5722.
(46) Kang, S.-W.; Ko, D.-H.; Kim, K. H.; Ha, D.-C. *Org. Lett.* **2003**, *5*, 4517.
(47) Rudolph, J.; Schmidt, F.; Bolm, C. *Adv. Synth. Catal.* **2004**, *346*, 867.
(48) Lu, G.; Kwong, F. Y.; Ruan, J.-W.; Li, Y.-M.; Chan, A. S. C. *Chem. - Eur. J.* **2006**, *12*, 4115.

DOI: 10.1021/acs.joc.5b01766
J. Org. Chem. 2015, 80, 10163−10176